Jimma University

Jimma Institute of Technology

Faculty of Mechanical Engineering

Thermal Systems Engineering

Performance Analysis of Heat Transfer Using Nanofluid for Indirect Solar Thermal Injera Baking with Storage System

By

Eyosiyas Yohannis

Presented in Partial Fulfillment of the Requirements for the Degree of Masters of Science in Thermal Systems Engineering

January 2020

Jimma, Ethiopia

Jimma University

Jimma Institute of Technology

Faculty of Mechanical Engineering

Thermal Systems Engineering

Performance Analysis of Heat Transfer Using Nanofluid for Indirect Solar Thermal Injera Baking with Storage System

By

Eyosiyas Yohannis

A Thesis Submitted to faculty of Mechanical Engineering

Presented in Partial Fulfillment of the Requirements for the Degree of Masters of Science in Thermal Systems Engineering

Advisor: Balewugize A. Zeru (Assistant Prof.)

Co advisor: Nebiyu Bogale (Assistant Prof.)

January 2020

Jimma, Ethiopia

DECLARATION

This thesis is my original work and has not been presented for a degree nor published in any other university or journals.

Name: - Eyosiyas Yohannis Kussa

_____ _____

Signature Date

Approved by

Name: - Balewgize A. Zeru (Assistant prof)

_____ _____

Advisor Date

Name: - Nebiyu Bogale (Assistant prof.)

_____ _____

Co-Advisor Date

Name: -Getachew S. Tibba (Dr.-Ing.)

_____ _____

External Examiner Date

Name: -Tarekygn Limore (MSc)

_____ _____

Internal Examiner

Name: -; -Fikadu Kifle (MSc) Date

_____ _____

Chair

ACKNOWLEDGEMENTS

First, I would like gratefully acknowledge the Almighty God for his help. My deepest gratitude goes to my advisor Mr. Balewgize A. Zeru, my co-advisor Mr. Nebiyu Bogale for all their limitless efforts in guiding me through my work. Finally, my deepest appreciation goes to Jimma University, School of Graduate Studies, Jimma Institute of Technology, faculty of mechanical engineering, thermal system engineering chair holder and staffs.

Abstract

The main energy source of developing countries for cooking comes from biomass. Like most developing countries, Ethiopia is also dependent on using traditional fuels. More than 98% of its household energy comes from biomass and less than 2% from electricity and petroleum collectively [9]. The biomass energy is mainly used to bake the country's common food type called "Injera" and its stew [41]. Solar energy is also can be used as energy source for baking process but, it requires efficient collection and working fluids with high heat transfer characteristic. The fluids used on the design of solar thermal injera baking process were shell Thermia oil B and steam. Shell Thermia oil B have low thermal property this could increase the time required for the baking process and the size of the components. Steam was also used as working fluid but, during operation the pressure on the pipes would develop up to 40 bar and due to condensation of the steam corrosion could happen on the wall of pipe. this reduces the life of the system

The main objective of this research was to study the performance of solar thermal Injera baking system using nanofluid as heat transfer. Nanofluid used was Cu/shell Thermia oil B with a volume concentration of 4% of nanoparticle. Thermo-physical property for nanofluid was calculated using theoretical models obtained from the literature. Phase change material was integrated into the system to allow night-time baking. Nitrate salt ($40\%KNO_3$-$60\%NaNO_3$*) was used as energy storage material due to its highest melting temperature (*222^0C*). Parabolic trough collector used to collect heat from solar radiation using heat transfer fluid and amount of heat collected was transported to the Injera baking pan and storage material through the piping system. The Pump was used to circulate the fluid through the system. Part of fluid was stored below the pan to control temperature fluctuation on the surface of the pan and keep the system at steady condition during baking.*

CFD simulation was done to determine the heat-up time and charging time for baking pan and PCM respectively. Also, the performance of heat transfer fluid for nanofluid and shell Thermia oil B was compared based on the simulation results. Simulations show that heat up time for the baking pan was enhanced by 43.6% using nanofluid and maximum temperature on the surface of the pan was registered 195^0 C. *The use of nanofluid reduced charging time for PCM by-30.6%.*

***Key words**; nanofliud, Phase change material, Injera, CFD Simulation.*

Table of Content

List of Figures

List of Tables

List of Symbols

A_p	Area of pan (m^2)
Ar	Area of receiver (m^2)
C_f	Specific heat capacity of base fluid (J/g. k)
C_{nf}	Specific heat capacity of nanofliud (J/g. k)
C_{pan}	Heat capacity of pan (J/g. k)
CR	Concentration ration
D	Diameter of pan (m)
dT	Temperature change (K)
Dc	Diameter of PCM cylinder (m)
d_p	Diameter of the nanoparticle (mm)
d	diameter of the pipe (mm)
Eu	Energy utilized on cooking Injera (J)
f	Parabola focal distance (m)
Gr	Grashof number
H	Monthly average dailyglobal radiation on horizontal surface(MJ/m^2. day)
H_O	extraterrestrial radiation for the location averaged over the time period (MJ/m^2. day)
ΔH	Melting enthalpy (J/g)
H_g	Height of oil gallery (m)
hc	Convective heat transfer coefficient (W/m^2.k)

hr	Radiation heat transfer coefficient (W/m^2.k)
H_c	Height of the PCM cylinder (m)
g	Gravity ($\frac{m}{s^2}$)
Gr	Grashof number
Isc	solar constant (W/m^2)
Isc	solar constant (W/m^2)
Ib	Beam radiation (W/m^2)
K	Thermal conductivity (W/m.K)
K_f	Thermal conductivity of base fluid (W/m.K)
K_{nf}	Thermal conductivity of nanofliud (W/m.K)
K_T	Monthly Average Daily clearness index
L_c	Characteristic length (m)
LP	length of the pipe (m)
m	mass (Kg)
$\dot{m}$	Mass flow rate (Kg/s)
N_u	Nusselt number
Pr	Prandtl number
P	Perimeter of the heat transfer pan surface (m)
Ped	Peclet number
Q	Energy stored (J)
Qh	Heat up energy (J)
Qt	Total amount of energy (J)

$\dot{Q}$	Heat transfer rate (W)
Qs	Solar energy on the collector aperture (J)
Ra	Rayleigh number
Re	Reynolds number
T_i	Initial temperature (K)
T_f	Final temperature (K)
T_m	Melting temperature (K)
T_{boil}	Boiling temperature of water (K)
t	Time (S)
T_r	Temperature of receiver (K)
T_{in}	Fluid inlet temperature (K)
T_o	Outlet temperature (k)
T_{co}	Receiver cover outer surface temperature (k)
T_{ci}	Receiver cover inner surface temperature (k)
u_m	Mean velocity of the fluid (m/s)
VT	Total volume of oil gallery (m^3)
W	Aperture width (m)
αnf	Thermal diffusivity of nanofliud
βnf	Volumetric thermal expansion of nanofliud
δ	Declination (^{0})
β	liquid fraction
μ	Dynamic viscosity (kg/m.s),

μ_{nf}	Dynamic viscosity of nanofliud
μ_{f}	Dynamic viscosity of base fluid
ν	kinematic viscosity (m^2/s)
θm	Half acceptance angle
ρ	Density (Kg/m^3)
ρ_{nf}	Density of nanofliud (Kg/m^3)
ρ_{f}	Density of base fluid (Kg/m^3)
φ	Latitude(^{0})
ωs	Sunset hour angle (^{0})
∅	Volume concentration of nanofliud
$\boldsymbol{\varphi_r}$	Rim angle

CHAPTER ONE

INTRODUCTION

1.1 Background

The main energy source of developing countries for cooking application comes from biomass. Studies show about 800 million people who are dependent on this form of energy are exposed to death and critical health problems. This is worse in the Sub-Saharan Africa (SSA) region where there is high biomass energy demand with a steady population growth. It accounts for 70 % to 90 % of primary energy for most SSA countries. The energy estimation of 2030 shows one billion Africans will depend on traditional biomass and half a million will die from its impact [9].

Like most developing countries, Ethiopia is also dependent on using traditional fuels. More than 98% of its household energy comes from biomass and less than 2% from electricity and petroleum collectively. The biomass energy is mainly used to bake the country's common food type called "Injera" and its stew. Injera is commonly prepared from "Teff" (Eragrostis tef), and is consumed two to three times per day by most household. Generally, more than 50% of the biomass fuel is used to bake this food item. The kitchen used to bake Injera is highly polluted with smoke, soot, and products of incomplete combustion. The use of biomass fuel in a traditional stove has been affecting the health and school time of millions of women and children. It also puts pressure on the country's forest coverage leading to erosion and land degradation [41].

Injera is spongy flat bread with a distinctive test and texture. It is predominantly eaten as staple food item in Ethiopia and some parts of East Africa. It is similar to an Indian Chapatti with small bubbly structures or eyes on top. In most households of Ethiopia, the energy demand for baking Injera is largely met with bio-mass such as: fuel wood, agricultural residue and dung cakes. Whereas, electricity is used in some of urban households [8].

Recent energy crises motivated researchers to improve the stove efficiency and its possibility to work with other alternative energies such as biogas and solar. Solar energy is one of the most promising renewable energy sources since it is free, available at all locations, and non-polluting.

This paper will address possibility of the high temperature indoor solar cooking, night cooking and reduced initial heating up time by using Nano fluid as heat transfer fluid. The enhancement of heating or cooling may create a saving in energy, reduce process time, raise thermal rating and lengthen the working life of equipment. Heat transfer efficiency can also be improved by increasing the thermal conductivity of the working fluid. Commonly used heat transfer fluids such as water, ethylene glycol, and engine oil have relatively low thermal conductivities, when compared to the thermal conductivity of solids. Nano fluid is a new kind of heat transfer medium, containing nanoparticles (1–100 nm) which are uniformly and stably distributed in a base fluid. These distributed nanoparticles, generally a metal or metal oxide greatly enhance the thermal conductivity of the Nano fluid, increases conduction and convection coefficients, allowing for more heat transfer.

Solar energy collectors are special kind of heat exchangers that transform solar radiation energy to internal energy of the transport medium. This is a device which absorbs the incoming solar radiation, converts it into heat, and transfers this heat to a fluid (usually air, water, or oil) flowing through the collector. The solar energy thus collected is carried from the circulating fluid either directly to the hot water or space conditioning equipment, or to a thermal energy storage tank from which can be drawn for use at night and/or cloudy days. There are basically two types of solar collectors: non concentrating or stationary and concentrating. A non-concentrating collector has the same area for intercepting and for absorbing solar radiation, whereas a sun-tracking concentrating solar collector usually has concave reflecting surfaces to intercept and focus the sun's beam radiation to a smaller receiving area, thereby increasing the radiation flux. Injera baking process requires large amount of temperature $180^0C - 220^0C$ [9]. In order to deliver high temperatures with good efficiency a high performance solar collector is required. Systems with light structures and low cost technology for process heat applications up to 400^0C could be obtained with parabolic through collectors (PTCs). PTCs can effectively produce heat at temperatures between 50^0C and 400^0C[42].

1.2 Statement of the problem

The most abundant energy source for cooking purposes in Ethiopia is biomass and the majority of this energy goes into the injera baking process. During the traditional biomass Injera baking process kitchen environment is highly polluted with soot and smoke that affect the health of household inhabitants. In addition to that, it will highly contribute to climate change. The source for fuelwood is forest and due to deforestation, desertification and soil degradation will happen. Another alternative source for injera baking is electricity but it has high fluctuation and not available in rural area. Solar energy is used as energy sources for injera baking process. The use of solar energy reduces the problem mentioned above but, it requires efficient collection and transferring. Solar thermal injera baking process uses solar radiation as an energy source to heat the fluid circulating through the system. The efficiency of the system depends on the thermal properties of the fluid circulating through the system and geometry of the heat collecting elements. Conventional fluids used on the design of the solar thermal injera baking method were shell Thermia oil B and steam. Shell Thermia oil B has low thermal properties, this would reduce the heat transfer performance of the system. Due to the low thermal property of the oil, the time required to raise the temperature of the pan from room temperature to the baking temperature was large (heating uptime) and the size of the system is not compact. Steam was also used as a working fluid for the solar thermal injera baking method but, the pressure on the system could develop up to 40 bar and condensation of the steam corrode the pipes. Due to those problems, the life of the system could be reduced. Heat transfer property of the fluid can be enhanced by enhancing the thermophysical properties of the base fluid. Suspended small solid particles on the base flued enhance the thermal property of the fluid. Fluid containing suspended colloidal nanoparticle have been called as nanofluid. There are different kinds of nanoparticles metallic or metal oxide. In this thesis nanofluid used is Cu/shell Thermia oil B (copper nanoparticles and shell Thermia oil is base fluid). So, the improvement of the thermal property of the base fluid is required to improve the heat transfer characteristics and reduces the size of the components.

1.3 Motivation

Conventional fluids such as water and shell Thermia oil B were used for design of solar thermal injera baking process. The low heat transfer performance of these conventional fluids obstructs the performance enhancement and the compactness of components. The effective performance of the system mainly depends on the heat transfer property of the working fluids. The thermal conductivity of the heat transfer fluids plays a vital role in the development of energy efficient heat transfer equipment. Thermal conductivity of liquids is typically orders of magnitude lower than that of solid. Thus, it is natural to consider improvement of thermal properties of conventional heat transfer fluids by addition of solid particles. Nanofluids are a modern class of colloids, in which typically solid particles with a very small diameter of 1-100 nm are suspended in a liquid medium. This addition of small sized particle on the base fluid enhance thermal conductivity and convective heat transfer performance.

1.3 Objectives

1.3.1 Main objective

The main objective of this thesis is performance study of heat transfer using Nano fluid for indirect solar thermal injera baking with PCM storage system.

1.3.2 Specific objectives

- To design solar parabolic trough collector and perform heat transfer analysis on the receiver.
- To design and model energy storage material.
- To perform CFD analysis during the initial heating time for injera baking process using nanofluid and conventional fluid.
- To perform CFD analysis for PCM

1.4 Significance of the Thesis

In Ethiopia more than 80% of people living in the rural area whose energy source mainly depends on firewood, animal dung, and crop residues. The main problem related to those energy sources are;

- Wastage of time during the collection.
- Health-related problems during the burning of firewood, animal dung and crop residues (highly contribute to the global warming and air pollution).
- Reduces large heating time required.

So, the solar baking system will solve those problems due to its dominant availability and pollution -free. It also reduces air pollution and deforestation

1.5 Scope of the study

The scope of this research was design and modelling of components such as parabolic trough collector, phase change material, pan and oil gallery assembly.CFD analysis was performed by using ANSYS 16.0. The aim of CFD analysis was to obtain heat up time required to raise the surface temperature of the baking pan from the ambient temperature to the baking temperature required by injera and to determine charging time of PCM material.

CHAPTER TWO

LITERATURE REVIEW

2.1 Background

The current energy regime in Ethiopia, one that is heavily reliant on the burning of biomass, has had major implications for the environment. The use of traditional fuels as the main source of energy by rural households, which comprise the vast majority of Ethiopia's population, is especially an area of concern. Deforestation, land degradation, decreases in agricultural productivity, and increased greenhouse gas emissions have resulted from these patterns of unsustainable fuel consumption, and are further exacerbated by Ethiopia's growing population's increased energy demands [1]. Due to this problem using renewable energy as a power source is the only solution. Ethiopia is known to have an annual mean average solar radiation of about, $5.2 kWh/m^2$, with the minimum being $4\ kWh/m^2$and the maximum estimated to be $6\ kWh/m^2$.With this solar radiation it is possible to collect enough energy for water heating, cooking application and generating electricity [2].

Based in the data obtained from the meteorology agency average solar radiation, for the Jimma is around $5.67 kWh/m^2$ day and the detail for calculation is included on the following section

2.2 Solar thermal collector

Radiant energy from the sun is converted to heat energy through special kind of heat exchanger called solar thermal collector. It uses heat transfer fluid (water, air and oil) to convert radiation energy to heat energy. Basically solar thermal collectors are classified into two [3].

a) Non Concentrating or stationary; has the same area for intercepting and for absorbing solar radiation.
b) Concentrating or sun tracking; Has concave reflecting surfaces to intercept and focus the sun's beam radiation to a smaller receiving area, thereby increasing the radiation flux.

Table 2. 1 Solar energy collectors [3]

Motion	Collector type	Absorber type	Concentration ratio	Indicative temperature range (^0C)
Stationary	○ Flat plat collector (FPC) ○ Evacuated tube collector (ETC) ○ Compound parabolic collector (CPC)	Flat Flat Tubular	1 1 1-5	30-80 50-200 60-240
Single axis tracking	○ Linear Fresnel reflector (LFR) ○ Parabolic trough collector (PTC) ○ Cylindrical trough collector (CTC)	Tubular Tubular Tubular	10-40 15-45 10-50	60-250 60-300 60-300
Two axes tracking	○ Parabolic dish reflector (PDR) ○ Heliostat field collector (HFC)	Point Point	100-1000 100-1500	100-500 150-2000

From the above classification of collector parabolic trough collector, is selected for this system. The temperature required at the outlet of the collector absorber is 260^0c so this amount of temperature is attainable by using solar parabolic trough collectors. It can produce heat at the temperature range of 50^0c up to 400^0c.Structurally it is light and low cost. PTCs are made by bending a sheet of reflective material into a parabolic shape. A metal black tube, covered with a glass tube to reduce heat losses, is placed along the focal line of the receiver. PTCs focus direct solar radiation onto a focal line on the collector axis. PTCs can only use direct solar radiation, called beam radiation or Direct Normal Irradiance (DNI), i.e., the fraction of solar radiation that is not deviated by clouds, fumes or dust in the atmosphere and that reaches the Earth's surface as a parallel beam.PTC used for solar power plant operate at the temperature range of $300^0c - 400^0c$ .Typical aperture width for 6m, total length from 100 to 150m and geometric concentration

relies between 20 and 30.It is also used for industrial process heating domestic water heating and space heating($100^0c - 250^0c$).Aperture area required for this range of temperature is between 1-3m and total length varies between 2-10m with geometric concentration relies between 15-20[45].

2.3 Injera baking method in Ethiopia

Injera is flat bread with a unique taste (sour and tasty) having spongy like structure with thickness of 2-4mm and most commonly with diameter of 58cm. Prepared from teff and mixture of other cereals like sorghum, barley rice and wheat [4].

Most common food at east Africa (Ethiopia, Eretria, Somalia and Sudan). Most Ethiopians eat Injera at least two times a day and it is being exported to North America and Middle East

Prepared by mixing flour (pure teff or mixture with other cereals) with water and left to ferment for two to four days. If the location is warm it will ferment with less day. Starter (left-over batter from the previous baking time) may be added to trigger fermentation. Approximately four to six hours before baking, a layer of bitter fermentation product is removed and hot water is added to reactivate fermentation, then the batter is poured on top of the hot baking pan surface [5].

Injera baking method is classified in to four based on the source of energy

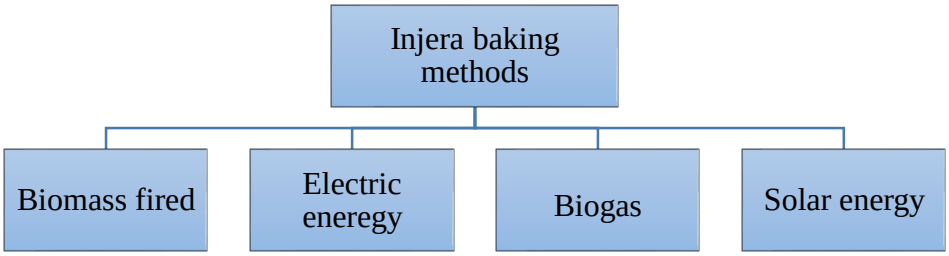

Figure 2. 1 Injera baking methods

2.3.1 Biomass injera baking method

The heat supplied to the baking pan is comes from biomass like wood, agricultural products and solid waste. Traditionally it uses open fire system which uses three stones to support the pan but this method of baking has high energy lost. Less amount of heat is transferred to the pan, inefficient and wasteful; and also is unhealthy because of carbon inhalation to the lungs and irritation of eyes. Due to those problems people modified this system in to mirte stove [4, 5].

a) b)

Figure 2. 2 a) open fire stove b) mirte stove

2.3.2 Electric injera baking method

This method is mainly used on the urban area where electric power is available. It reduces problem that mentioned on the biomass fired system but it has great problem of fluctuation and availability since most number of people living on the rural area in Ethiopia [5].

a) b)

Figure 2. 3 a) Electrical Injera baking stove b) biogas Injera baking stove

2.3.3 Biogas injera baking method

Biogas is the mixture of gases produced by the breakdown of organic matter in the absence of oxygen(anaerobically), primarily consisting of methane and carbon dioxide. Biogas can be produced from raw materials such as agricultural waste, manure, municipal waste, plant material, sewage, green waste or food waste. Combustion of methane using proper fuel-to-air ratio will

create a non-polluting and comfortable kitchen for injera baking. biogas injera baking stove as shown in fig 2.3 (b) contains three concentric rings made from the steel pipe [4].

2.3.4 Solar thermal injera baking method

In solar thermal injera baking method the radiant energy from the sun is converted to the heat energy by using solar collector and this heat energy is circulated through the system by heat transfer fluid. So many people did research on this area starting from the design and developmental of the system to the improvement of the system efficiency.

Abdulkadir et al. [6], the performance of injera baking pan for indoor cooking is studied on this paper. The system works by the principle of transferring solar thermal energy in to the kitchen by heat transfer fluid. They manufactured ceramic pan and it has steel pan below it with fin with the purpose of increasing heat transfer and preventing the contact between the fluid and pan. Some amount of oil is stored below the pan in order to overcome a sudden drop of baking pan top surface temperature below the optimum temperature range. From their experimental result, they were observed that it took approximately 1hour for heating oil to 300^0C and 40 minutes to reach the optimum baking surface temperature. Injera is removed from the baking pan every two minutes and it takes an idle time of three minutes between each injera to recover to optimum baking temperature. Based on average family size, 20 injera can be baked per day in approximately three hours and 28 minutes.

Abdulkadir A. Sisay B. et al. [7], investigated the probability of baking injera by glass pan. Solar thermal energy transferred to the kitchen by means of a circulating heat transfer fluid heated by solar energy concentrated by a parabolic trough. The existing three stone biomass-based clay baking pan results in a loss of a major portion of the supplied energy and the baking process also result in significant amounts of indoor air pollution. They used an electric heater for simulation purposes and obtained 191^0C temperature on the surface of the pan.

Hassen and Amibe [8], developed a finite element model for solar- powered injera baking oven for indoor cooking. They used 8mm thickness ceramic pan for their investigation and study the heat-up time and temperature distributions during initial heat-up and cyclic baking of the new model. Finally, they concluded from their simulation result that the heat up time can be reduced by reducing the thickness of the baking pan for a given supply oil temperature. There is also a

significant reduction in the idle period by reducing the thickness of the baking pan or by improving the supply oil temperature. This baking system gives reasonable heat up and baking time for 8mm thick ceramic pan with a heated oil temperature of $275\ ^0C$.

Asfafaw et al. [9], introduced a new injera baking solar thermal method which use the direct steam to heat the surface of the baking pan. The heat transfer process has been governed by the principle of natural circulation boiling-condensation between receiver and stove. Their experimental result shows that the quality of Injera in the range of 135-220^0C remains the same, however, a slightly baking time difference was observed. During their experiment they obtained three results. The first result shows direct solar steam-based baking i.e.; it proves indoor solar baking is possible. Secondly, Injera baking using solar energy was impossible due to its high-temperature demand; this study can change this attitude and encourage researchers to go for improved indirect high - temperature solar cookers in general. The third and important result is the possibility of Injera baking at 135-160^0C that will bring a significant impact in the revolution of the injera stove in Ethiopia.

Tesfay [10], developed an injera baking off-focus system. In addition to the off-focus solar thermal application, they discussed the integration of solar thermal with heat storage for sustainable future use. The prototype for direct steam - based baking was developed and tested in Mekelle University (Ethiopia) and Phase change material based heat storage prototype was developed and tested at NTNU. Both experiments showed the possibility of solar energy for Injera baking and its sustainability by including latent heat storage

2.5 Thermal energy storage

A thermal storage can significantly increase the performance and competitiveness of a solar installation. Solar irradiation is intermittent and irregular, so a storage can correct this variation to optimize the use of the energy collected**.**

2.5.1 Thermal energy storage methods

There are three methods for storing thermal energy.

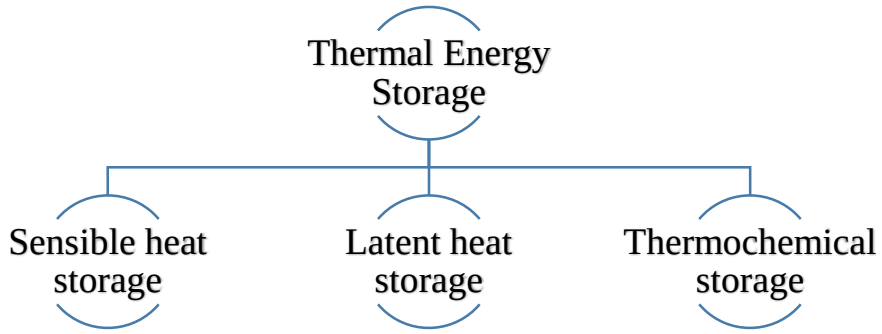

Figure 2. 4 Thermal energy storage methods

2.5.1.1 Sensible heat storage

A method of storing energy without causing a phase change on material. Energy stored due to increase of temperature on the material. Amount of energy stored depends of specific heat, temperature change and the amount of material. [11]

$$Q = \int_{Ti}^{Tf} mcp(dT) \tag{2.1}$$

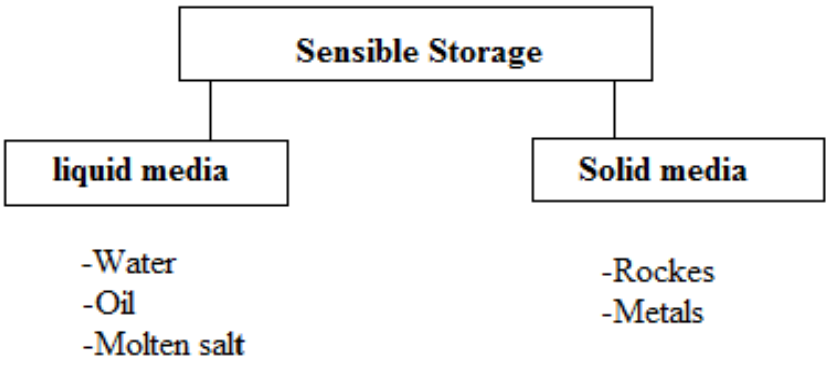

Figure 2. 5 Sensible energy storage methods

2.5.1.2 Latent heat storage

Latent heat thermal energy storage (LHS) involves heating material until it experiences a phase change, which can be from solid to liquid or from liquid to gas; when the material reaches its phase change temperature it absorbs a large amount of heat to carry out the transformation, known as the latent heat of fusion or vaporization depending on the case, and in this manner the energy is stored. [11]

$$Q = \int_{Ti}^{Tm} mcp(dT) + m\Delta H + \int_{Tm}^{Tf} mcp(dT) \qquad (2.2)$$

Asfafaw etl. Were studied charging and discharging of phase change material heat storage using steam as working fluid. PCM they used to be nitrite salt which was a mixture of 60%NaNO_3 and 40% KNO_3. The storage has charged on successive days using the advantage of materials heat retention ability by using energy from the sun with circulating steam temperature of 250^0C.Also they charged the material with an artificial heater with the surface temperature maintained at 450^0C and obtained charging time of 8 hours [40]. Maxime et al. [12]**,** were studied different types of high- temperature thermal storage materials. The range of temperature studied was between 180 and 250^0C. A comparison between the best sensible heat materials (iron, carbon) and melting materials (nitrate salts, tin) is realized to conclude on the relevance of latent heat-based system compare to sensible heat-based ones. For latent heat storage, Potassium-Sodium nitrate salts (KNO_3− NaNO_3) and tin were used with the melting temperature of 220^0 and220^0 consecutively. For the sensible heat materials, two different materials will be studied: iron, which has been chosen because of its high volumetric and slightly increasing sensible heat regarding the temperature and graphite, because of its significantly increasing sensible heat regarding the range of temperature. Finally, they obtained that Total heating time is much shorter for the latent heat-based system and by comparison of the heat capacities the latent-heat based systems are more effective than the sensible-heat.

2.5.1.3Thermochemical storage

The principle of a thermochemical heat storage is to use the energy from an exothermic reaction for the application, and charge the storage by running the corresponding endothermic reaction. The

storage potential of the thermochemical energy is very important, but the technical limits are nowadays too high to be suitable for a low-cost solar cooking system. [11]

2.5.2 Phase change materials used on high temperature application

Selection of phase change material for the energy storage depends on the variety of properties.

- Phase change temperature of material it should be near to operating temperature
- Latent heat of material it should be high to minimize volume of size
- High specific heat to store additional heat
- High thermal conductivity on both state
- High density, small volume changes at both solid and liquid phase
- Should not be toxic, flammable, or explosive

Some of solar salts that are used as PCM material were presented on table 2.2 and the best PCM for the proposed system will be selected.

Table 2. 2 properties of PCM [18]

PCM	Melting temperature(C)	Melting enthalpy(J/g)	Thermal conductivity(w/m.k)		Specific heat capacity (J/g.k)		Density (g/cm^3)
			Solid	Liquid	Solid	liquid	
NaNO_2	270	200	0.96	0.54	1.8	1.6	2.17
NaNO_3	306	175	0.59	0.57	1.78	1.8	1.9
KNO_3	337	100	-	0.4	1.43	1.46	1.85
60% NaNO_3 - 40% KNO_3	222	100	-	0.5	1.42	1.53	1.95

2.6 Nanofliud

Nanofluid are colloidal suspensions of Nanosized solid particles in a liquid. Recently conducted experiments have indicated that Nanofluid tend to have substantially higher thermal conductivity than the base fluids [13]. Among the many advantages of Nanofluids over conventional solid-liquid suspensions, the following are worth mentioning.

- Higher specific surface area
- Higher stability of the colloidal suspension
- Lower pumping power required to achieve the equivalent heat transfer
- Reduced particle clogging compared to con-ventional colloids
- Higher level of control of the thermodynamics and transport properties by varying the particle material, concentra-tion, size, and shape [13].

Dharani Kumar et al. [14], experimentally studied the effect of Nanofluids and absorber tube geometry on the heat transfer process. They modified absorber tube with copper fins and using (T TiO_2) Nanofluid with (0.5g and 1 g) concentration. They obtained various results with changing the Nano fluid concentration outlet temperatures are measured and without the addition of Nano fluids outlet temperatures are measured. They described that the outlet temperature increases with increases in Nanofluid concentration and also Fins are used to increases the surface area so that the heat transfer rate increases**.**

Dimitrios Korreset et al. **[15]** did an investigation of a Nanofluid-based compound parabolic collector under laminar flow condition. The examined Nanofluid is Syltherm 800/CuO with 5% volumetric nanoparticle concentration and the examined temperature range is from 25^0C up to 300^0C. From the results they concluded that the use of Nanofluid-based CPC is most appropriate at higher temperature levels where the thermal efficiency enhancement is higher and also there is exergy efficiency enhancement. The application of Nanofluids increases the flow heat transfer coefficient by 15.53% for the low operating temperatures and up to 17.41% in the high operating temperatures. The mean heat transfer coefficient enhancement is 16.16%.

Azari1, et al. [16], studied experimental and Computational Fluid Dynamics (CFD) investigations of the laminar convective heat transfer coefficient of Al_2O_3/water Nano fluids in a circular tube under uniform and constant heat flux on the wall. Experimental and simulation results showed that the thermal performance of Nano fluids is higher than that of the base fluid and the heat transfer enhancement increases with the particle volume concentration and Reynolds number.

Ketan and Kundan [17], studied Experimental and CFD Investigation of the Parabolic Shaped Solar Collector Utilizing Nanofluid (CuO- H_2O and SiO_2 -H_2O) as a Working Fluid.ANSYS FLUENT 14.5 is used for carrying out CFD investigation. Nanofluids of SiO_2 -H_2O and CuO-H_2O of 0.01% volume concentration are used. From their experimental and CFD analysis they obtained Improvement in the efficiency of collector of about 6.68% and 7.64% is obtained using 0.01%vol. conc. SiO_2 -H_2O Nano fluid and 0.01% vol. conc. CuO- H_2O Nano fluid, respectively, as compared to H_2O at 40LPH while at 80 LPH improvement in efficiency of collector of about 7.15% and 8.42% is obtained using 0.01% vol. conc. SiO_2 -H_2O Nanofluid and 0.01% vol. conc. CuO- H_2O Nanofluid, respectively, as compared to H_2O.

2.6.1 Theoretical models used to calculate thermo physical properties of nanofliud

So many peoples did their studies on the determination of thermophysical properties of Nanofluids both analytically and experimentally. Some of the works will be summarized below.

Arul et al. estimated thermophysical properties of nanofliud by using theoretical models. They improved thermophysical properties of conventional fluids by suspending nanoparticles. Three base fluids (water, sodium and ethylene glycol) and three nanoparticles (Aluminum, Copper, and silver) were used in their study. Thermophysical Properties calculated by using theoretical models were density, specific heat and viscosity. Those properties are depending on various factors such as preparation method, Working temperature, particle size and shape, and volume fraction/concentration of nanoparticles.

Table 2. 3 theoretical model for specific heat and density [19]

No	Property nanofliud	Model
1	Specific heat (KJ/kg.k))	$\frac{(1-\emptyset)\rho_f C_f + \emptyset\rho_p C_p}{\rho_{nf}}$
2	Density (kg/m3)	$\rho_{nf} = (1-\emptyset)\rho_f + \emptyset\rho_p$
3	Thermal conductivity	$Knf = Kbf\left[\frac{Kp + 2Kbf - 2\emptyset(Kbf - Kp)}{Kp + 2Kbf + \emptyset(Kbf - Kp)}\right]$

Where ρ_{nf}=density of nanofliud, $\emptyset$=nanoparticle percent concentration, ρ_f=density of base fluid, ρ_p=density of nanoparticle, C_{nf}=heat capacity of nanofliud, C_f heat capacity of base fluid C_p heat capacity of nanoparticle

By using those theoretical models finally, they obtained that density of nanofliud increase with increasing concentration, specific heat of nanofliud decrease with increase of nanofliud and also dynamic viscosity increase with increasing particle concentration. Generally, they concluded that the thermo physical properties of nanofliud increase with increasing particle concentration. [19]

Additional thermo physical property models used by ching-chang et al. [20] on their numerical investigation of natural convection and entropy generation on the U-shaped cavity were given on the table 2.4.

Table 2. 4 Theoretical model for Prandtl number, dynamic viscosity and thermal diffusivity [20]

No	Property of nanofliud	Model
1	Prandtl number	$Pr = \frac{v_{nf}}{\alpha_{nf}}$
2	Dynamic viscosity	$\mu nf = \frac{\mu_{bf}}{(1-\emptyset)^{2.5}}$
3	Thermal diffusivity	$\alpha nf = \frac{k_{nf}}{(\rho cp)_{bf}}$

Supreeti Das [8] analyzed thermo physical properties of Nano fluid for heat transfer application such as heat exchanger and cooling systems. He defined Nanofliud as suspension of Nano sized

particle (1nm-100nm) on the base fluid that are used on different application. And also he suggested that volume fraction of nanoparticle under range of 2% up to 8% above this volume fraction will result on agglomeration and abrasions on the wall through which it is flowing. Finally, he proposed that possibility of designing lighter and compact heat exchanger by using Nano fluid due to the quantity required smaller than conventional fluids. Additional thermo physical property obtained from his paper is volumetric thermal expansion which is given as;

$$\beta nf = \frac{((1-\emptyset)\rho f \beta f + \emptyset \rho p \beta p}{\rho nf} \quad (2.3)$$

2.6.2 Types of nanoparticle

The thermo physical properties of nanofliud is mainly depends on the properties of nanoparticles. Types of nanoparticles investigated were;

- Pure metals (Au, Ag, Cu, Al, and Fe)
- Metal oxides (Al_2O_3, CuO, Fe_3O_4, SiO_2, TiO_2, and ZnO)
- Carbides (Sic, Tic)

Thermal conductivity of a liquid is an important physical property that decides its heat transfer performance.

Table 2. 5 Thermal conductivity of nanoparticles was given on the following table [44]

Types	Material	Thermal Conductivity ($Wm^{-1}k^{-1}$)
Metal	Gold	315
	Silver	424
	Copper	400
	Alumina	273
	Iron	80
	Steel	46
	Stainless steel	16
Metal oxide	Alumina(Al_2O_3)	40
	Cupric oxide	77
	Iron (I, II) oxide	8.37

	Zinc oxide	29

2.7 Heat transfer fluid used on solar thermal injera baking method

Heat transfer fluid used for indirect solar thermal injera baking method were shell Thermia oil B and steam. Shell Thermia oil B highly refined mineral oils and it have ability to provide superior performance in indirect closed fluid heat transfer system. It is used on industrial application such as process industry, chemical plants and textiles. It can be used in high temperature continues heat transfer equipment's with maximum film temperature of 340^0C and maximum bulk temperature of 320^0C.It has low viscosity (that enables excellent fluidity), noncorrosive and nontoxic [25].

2.8 Research gap

This thesis aimed to enhance the performance of the solar thermal injera baking system by using nanofluid as heat transfer fluid and also using PCM for night time baking purposes. The gaps observed on previous works were;

- Researchers were used shell Thermia oil B and steam as heat transfer fluid. The thermal conductivity of the oil is low due to this heat transfer rate from the fluid to the pan is low. This increases heat up time for injera baking pan. For the case of steam as heat transfer fluid the pressure on the piping system would develop up to 40 bar and due to condensation of the steam on the pipe corrosion could happen on the wall of the pipes. This could reduce the life of the system.
- Researchers also integrated latent heat storage system below the baking pan to store heat night time cooking purposes. But for this kind of integration, it was difficult to control heat flow from the storage to the pan, because of that direct contact of the baking pan bottom surface and PCM top part.

So, on this thesis it was aimed to use nanofluid as heat transfer fluid due to its high thermophysical property and PCM was separately integrated to the system. The Heat was transferred from the heating element to the baking pan through circulating fluids. Nanofluid used on this thesis paper is Cu/shell Thermia oil B. Copper has high thermal conductivity when compared with another nanoparticle, this will enhance the property of the nanofluid. Shell Thermia Oil B is used as a base fluid.

CHAPTER THREE

METHODOLOGY

3.1 Introduction

The primary research method for this study is literature review and conceptual modelling of the system. The main purpose of reviewing different papers related to proposed system is to obtain dates such as baking temperature of the injera, maximum temperature can be stored on the PCM and geometrical parameters for the pan suggested by different peoples (such as, diameters, thickness and height).

3.2 Location of Study area

The study area for the proposed system is Jimma, so the metrological data for solar collector design is will be obtained from Jimma national metrology agency. Jimma zone is located at southwestern Ethiopia that is located 335km by road southwest of Addis Ababa. Its geographical coordinates are between 7° 13'- 8° 56N latitude and 35°49'-38°38'E longitude with an estimated area of 19,506.24km^2. It lies in the climatic zone locally known as Woynā Dagā which is considered ideal for coffee agriculture as well as human settlement.

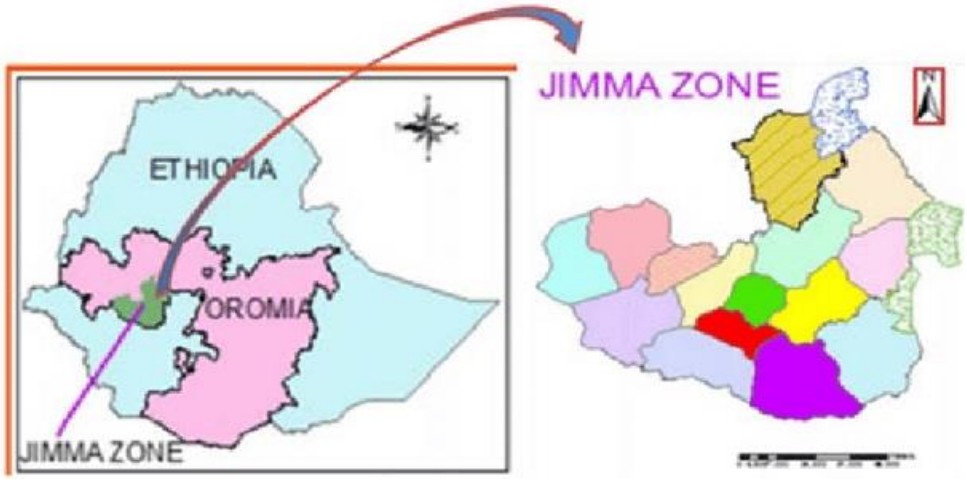

Figure 3. 1 Map of Jimma zone

3.3 Estimation of solar radiation

The utilization of solar energy, like any other natural resource requires detailed information on the availability of the amount of total solar radiation striking the earth surface. This total amount of solar radiation incidents on the earth's surface is called global solar radiation**.** Global solar radiation data are necessary at various steps of the design, engineering, simulation and performance evaluation of any project involving solar energy. The global solar radiation can be divided into two components**:** diffuse solar radiation, which results from scattering caused by gases in the Earth's atmosphere, dispersed water droplets and particulates; and direct solar radiation, which has not been scattered. Global solar radiation is the algebraic sum of the two components. [22]

So, on this paper the global radiation for Jimma will be analyzed by using daily sunshine hour obtained from meteorology agency. The data used for analysis were (2015-2017)

Table 3. 1 Sunshine hours

Parameters	**Months**	**2015**	**2016**	**2017**
SUNERS	01	8.09	7.15	9.07
SUNERS	02	7.05	7.2	6.9
SUNERS	03	8.3	7.54	7.76
SUNERS	04	7.8	5.02	8
SUNERS	05	6.74	5.58	6.12
SUNERS	06	4.3	4.65	5.97
SUNERS	07	5.06	3.2	3.23
SUNERS	08	4.75	4.64	3.99
SUNERS	09	6.4	5.75	5.15
SUNERS	10	8.8	8.5	6.7
SUNERS	11	7.2	7.9	7.55
SUNERS	12	6.73	8.25	8.66

Average sunshine hour 7 hours

Angles used to determine the direction of solar radiations are

a) Latitude (φ); - The angular location north or south of the equator, north positive;

$$-90^0 \leq \varphi \leq 90^0$$

b) Declination (δ); -The angular position of the sun at solar noon (i.e., when the sun is on the local meridian) with respect to the plane of the equator, north positive;

$$-23.45^0 \leq \varphi \leq 23.45^0$$

Declination angle can be found from approximate equation of cooper

$$\delta = 23.45sin(360\frac{284+n}{365}) \quad (3.1)$$

Where n is day of the year

Table 3. 2Reprsentative day of the year [13]

Months	**Day of the year**	**Representative day of the year**
January	17	January 17
February	47	February16
March	75	March 16
April	105	April 15
May	135	May 15
June	162	June 11
July	198	July 17
August	228	August 16
September	258	September 15
October	288	October 15
November	318	November 14
December	344	December 10

Based on the above data declination angle for each month is calculated

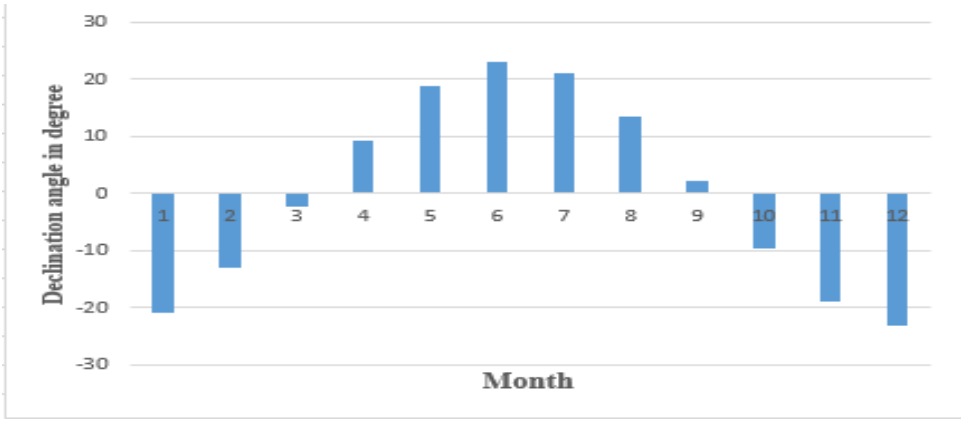

Figure 3. 2declination angle for each month

c) Solar hour angle; - is the angular displacement of the sun east or west of the local meridian; morning negative, afternoon positive. The solar hour angle is equal to zero at solar noon and varies by 15 degrees per hour from solar noon.

d) Sunset hour angle(ωs); -is the solar hour angle corresponding to the time when the sun set.it is given as

$$\omega s = cos^{-1}(-tan\varphi tan\delta)$$

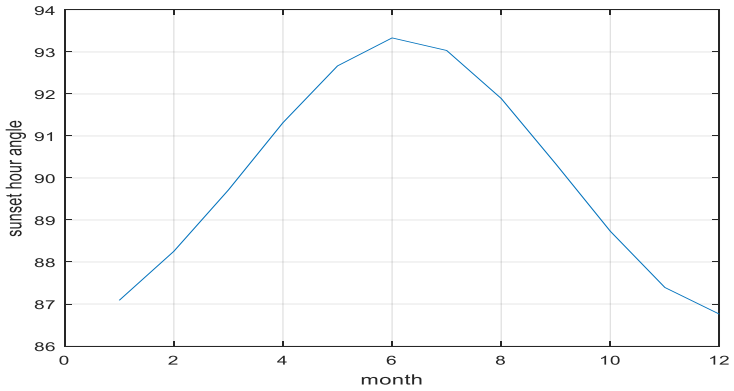

Figure 3. 3Sunset hour angle

3.4 Estimation of average solar radiation data

The original˚Angstr¨ om-type regression equation related monthly average daily radiation to clear-day radiation at the location in question and average fraction of possible sunshine hours

$$\frac{H}{Ho} = a + b(\frac{\bar{n}}{\bar{N}}) \quad (3.2)$$ Where

$H = monthly\ average\ dailyglobal\ \ radiation\ on\ horizontal\ surface(MJ/m^2.day)$

$Ho = extraterrestrial\ radiation\ for\ the\ location\ averaged\ over\ the\ time\ period$

$a\ and\ b = regression\ coefficients$ And obtained from the relation given below [22]

$$a = -0.11 + 0.235cos\varphi + 0.323(\frac{\bar{n}}{\bar{N}}) \quad (3.3)$$

$$b = 1.449 - 0.553cos\varphi - 0.694(\frac{\bar{n}}{\bar{N}}) \quad (3.4)$$

The monthly average daily extraterrestrial irradiation calculated as

$$Ho = 24/\pi Isc[1 + 0.0333cos(360 * n/365)][cos\varphi cos\delta cos\omega s + 2\pi\omega s/360 sin\varphi sin\delta] \quad (3.5)$$

Where Isc is the solar constant with numerical value of 1367 Wm^{-2}

$$\bar{N}=2/15\omega s \quad (3.6)$$

From the above equations the tables on APPENDIX A were generated for the three successive years

Table 3. 3 Monthly average daily global radiation on the horizontal surface for three years

Years	2015	2016	2017
Monthly average daily global radiations ($J/m^2.day$)	20776195.5	19895033.4	20288135.8

Taking the average value of three years the solar global radiation on the horizontal surface used for design is

$H=20.4\ \frac{MJ}{m^2Day}=5.67\ \frac{kWh}{m^2Day}$

The effective incident radiation measured on the plane of the aperture Ib includes only beam radiation for all concentrators except those of low concentration ratio (i.e., perhaps 10 or below). For systems of low concentration ratio, part of the diffuse radiation will be reflected to the receiver, with the amount depending on the acceptance angle of the concentrator [39].

This design uses a collector with high concentration ration so it conceders only beam radiation.

Monthly Average Daily clearness index (K_T);- Before reaching the surface of the earth, radiation from the sun is attenuated by the atmosphere and the clouds. The ratio of solar radiation at the surface of the earth to extraterrestrial radiation is called the clearness index [23].

$$\mathrm{K_T} = \frac{\text{daily total radiation}}{\text{daily extraterrestrial}} = \frac{\mathrm{H}}{\mathrm{Ho}} \tag{3.6}$$

$$K_T = \frac{\mathbf{20.4}}{35.5} = 0.57$$

Sunset hour angle (ωs) is greater than 81.4 degree so by using graph on APPENDIX F for the KT=0.57 $\frac{Hd}{H}$=0.35

$$Hd = 0.35 * \frac{5.67\mathrm{kWh}}{\mathrm{m2}}\,\mathrm{day} = \frac{1.9\mathrm{kWh}}{\mathrm{m^2}}.\mathrm{day}$$

$$\text{But,} \quad H = Hb + Hd$$

$$Hb = H - Hd$$

$$Hb = \frac{5.67\mathrm{KWh}}{\mathrm{m2.day}} - \frac{1.9\mathrm{kWh}}{\mathrm{m2.day}} = \frac{3.8\mathrm{kWh}}{\mathrm{m^2.day}}$$

Mean sunshine hour is taken from the average of three year = 7 hour

$$Ib = 3.8 * 1000 * 3600\mathrm{w/m2}\ /(7\ * 3600\mathrm{s}) = 630\mathrm{W/m^2}$$

3.4 System Description

The proposed system contains parabolic trough collector for heat collection, valves to control flow direction, pumps to drive fluids, phase change materials to store energy for night time baking purposes, temporary oil storage gallery. When radiation from the sun reaches the surface of the collector the fluid inside the absorber starts to absorb heat. pump I is used to drive fluid from the oil storage to the absorber and the fluid starts to flow through the absorber by absorbing heat from the collector. The system contains three loops, loop I is used to charging PCM, loop II is used to discharge PCM (night time cooking) and loop III, is used for day time baking of injera. Pump II is used to drive oil from the oil gallery to the storage and to discharging of PCM.in order to bake injera on the same way the baking pan should be kept in the temperature range of $(180^0C - 220^0C)$ for long time. In order to overcome sudden drop of baking pan top surface temperature below optimum range oil partly stored below the baking pan on the oil gallery. Solar panel is used to drive pumps and solar battery is used for night dive pumping process. Working principles is presented on fig 3.4.

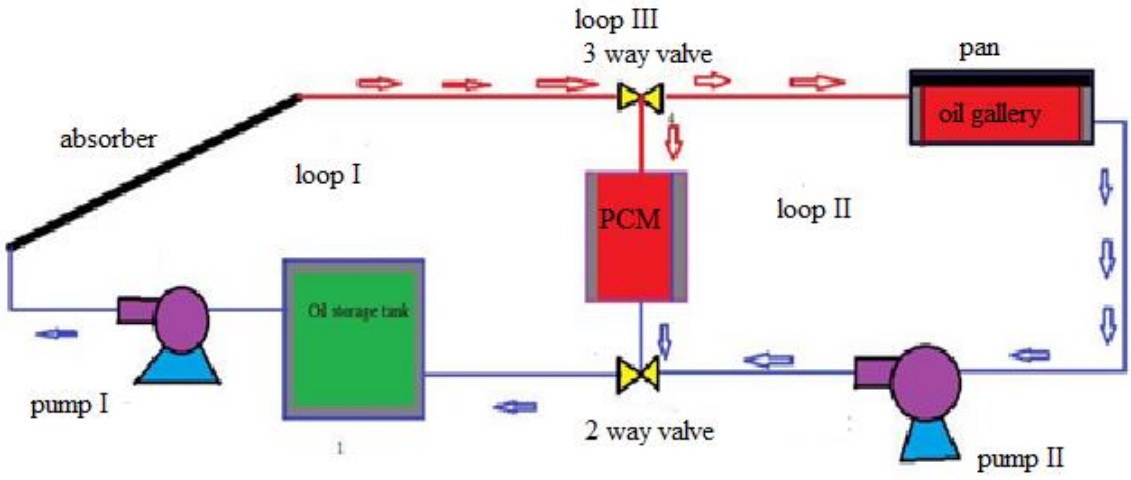

Figure 3. 4 System description

3.5 Computational fluid dynamics methodology

Computational Fluid Dynamics (CFD) is the science of predicting fluid flow, heat and mass transfer, chemical reactions, and related phenomena by solving numerically the set of governing mathematical equations. The use of CFD analysis for a given system is used to reduce the total effort and cost required for experimentation. ANSYS (fluent) is used to solve physical problems by using a finite volume method that discretizes a given demine into smaller control volumes to apply conservation equations.CFD code contains three main stages.

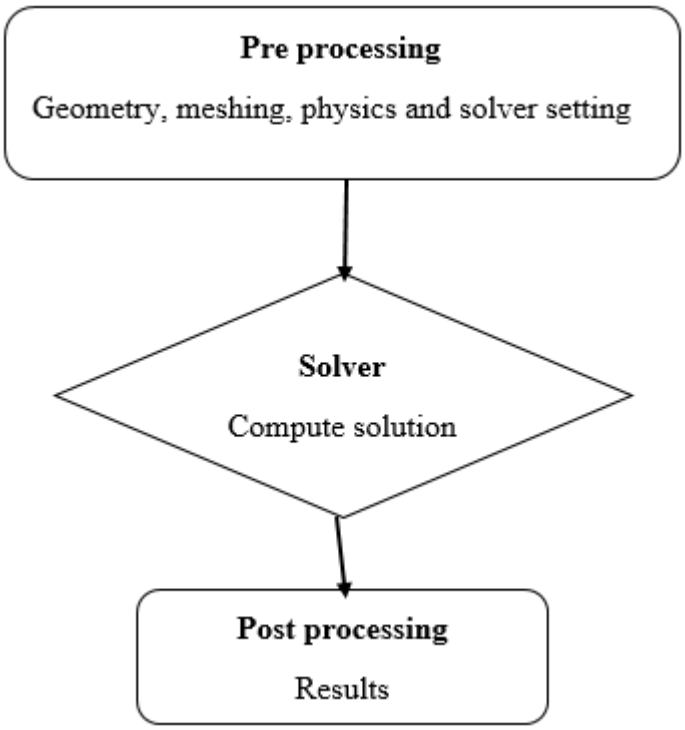

Figure 3. 5 CFD methodology

Pre processing

Geometry

On this step the geometry of the fluid domain and solid parts will be modeled. On this paper geometry of the injera baking pan assembled with oil gallery and PCM material on the storage cylinder are modeled

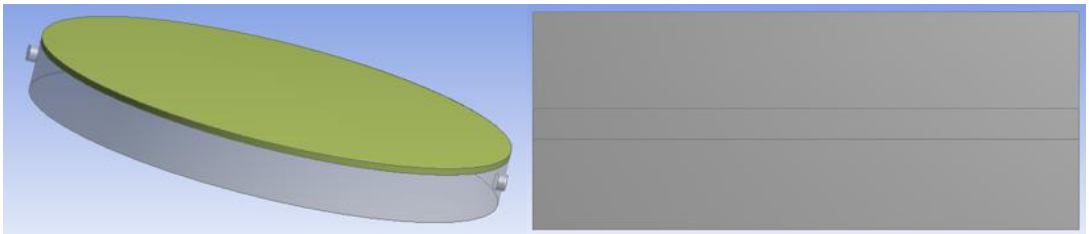

Figure 3. 6 CFD modelling

Mesh generation

Meshing is a method of dividing the flow domain into many elements or subdomains. Equations are solved in those domains. Different element types are available for 3D and 2D analysis, such as triangle and quadrilateral for 2D, tetrahedron, hexahedron and pyramid for 3D. For fig tetrahedron element type used and for fig quadrilateral element type is used. The presence of good meshing has a significant effect on the rate of convergence, solution accuracy and computation time. So the quality of meshing is cheeked by performing mess sensitivity analysis. Steady state analysis was used to check mesh sensitivity for oil gallery and pan assembly using two parameters temperature of the pan and storage.

Table 3. 4 Mesh sensitivity analysis for pan and oil gallery assembly

Mesh size(mm)	Pan Temperature (k)	Storage temperature (k)
15	483.67	569.8
10	494.96	569.63
5	506.68	569
3	506.7	568.69
1	506.92	568.92

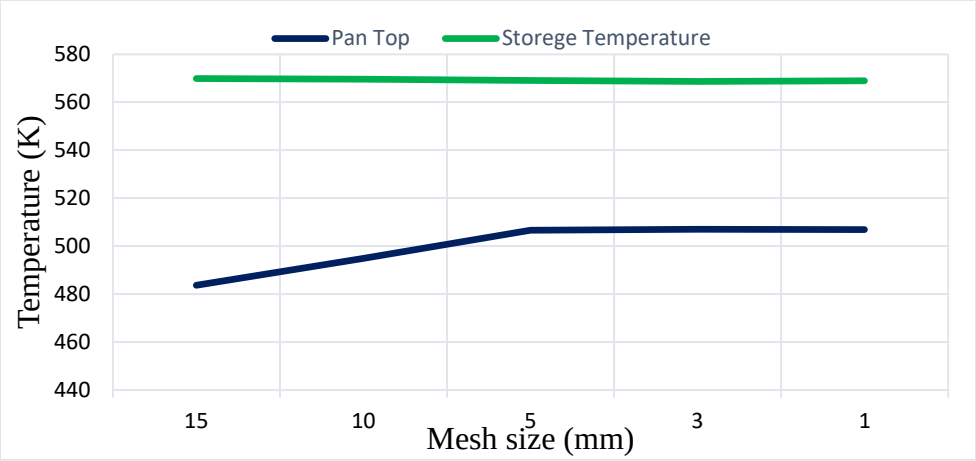

Figure 3. 7 Mesh sensitivity analysis for pan and oil gallery assembly

From figure 3.7 it was observed that there was no effect of mesh size on the study parameter after 5mm and the selected mesh size for this analysis was 3mm.

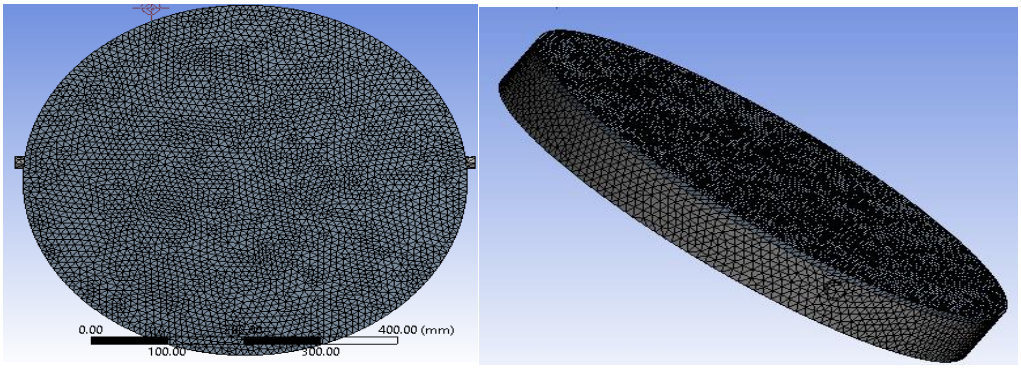

Figure 3. 8 Meshing of pan

Table 3. 5 Mesh sensitivity analysis for PCM

Mesh size [mm]	PCM temperature (k)	Outlet temperature (k)
10mm	304.94717	518.5846
5mm	308.62027	503.26312
3mm	309.29141	495.73276
2mm	309.4275	494.34382
1mm	309.62893	493.09969
0.5mm	309.8	310.11099

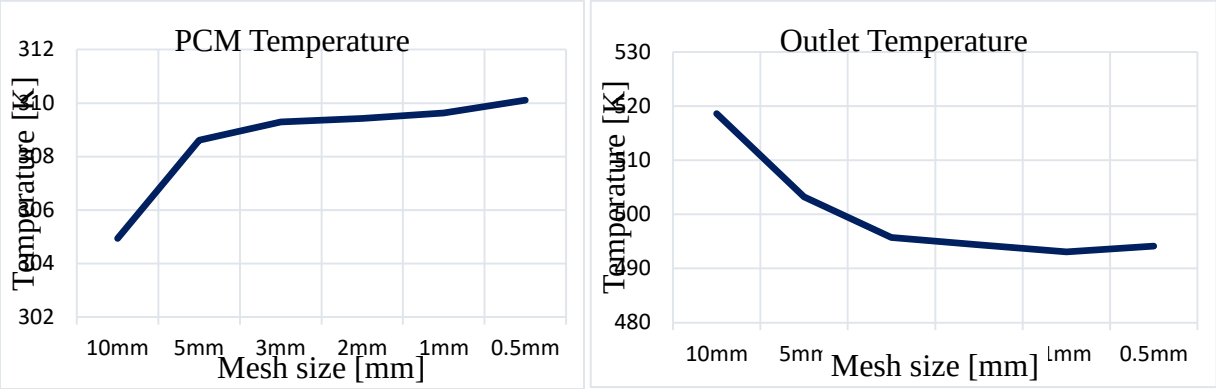

Figure 3. 9 Mesh sensitivity analysis for PCM

Mesh size selected for this analysis was 1mm and it was at good quality range

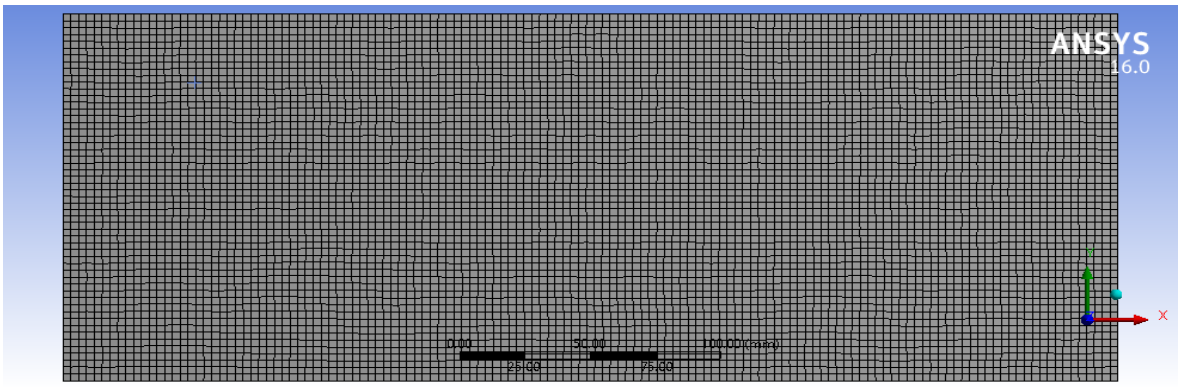

Figure 3. 10 meshing of PCM

.

Setup

ANSYS fluent contains two solver pressure- based and density- based. Historically speaking, the pressure-based approach was developed for low-speed incompressible flows, while the density-based approach was mainly used for high-speed compressible flows. For the simulation on this paper pressure-based solver was selected with the transient. Models used for simulation of injera baking with oil gallery were energy and viscous laminar flow and for PCM in addition to those model melting and solidification model used. Materials were selected as per requirements and boundary conditions were applied. Solution methods used for coupling of pressure and velocity were SIMPLE (semi-implicit method for pressure linked equations). The discretized conservation

equations are solved iteratively until convergence. Convergence was monitored by using residual scales. The convergence criteria of 10^{-6} was used for the residuals of the continuity equation, for the residuals of the velocity components and for the residuals of the energy equation is assumed. Before starting running the simulation it was initialized using standard initialization. Then selecting suitable time step and time step size /number iteration the system simulation was started.

Post processing; - Obtaining the results and visualization of the results.

CHAPTER FOUR

ENERGY AND HEAT TRANSFER ANALYSIS OF INJERA BAKING PAN

4.1 Energy consumption analysis of Injera baking pan (mittad)

Energy consumption of Injera baking pan is mainly depends on the thermo physical properties of pan (heat capacity, thermal conductivity …etc.). Those properties are obtained from literature reviews. Energy required in baking is defined as the amount of heat required to raise the temperature of batter from ambient to boiling point of water and vaporize portion of water on the batter. Total amount of energy is the summation of energy required for baking and heating the pan.

Energy utilized on cooking Injera

$$Eu = m_{batter} C_{pwater} (T_{boil} - T_{room}) + (m_{batter} - m_{injera}) h_{vaporization} \quad (4.1)$$

Where;Eu=energy utilized, m_{batter}=mass of batter=400g, m_{injera}=mass of injera which is 320g

C_{pwater} Specific heat capacity of water =4.187kJ/kg.k. This is due to heat capacity of batter is the same as that of water (batter contains 70% of water and 30% of cereals) [24]

T_{boil}=boiling temperature of water at Jimma which is 90.5^0C

T_{room}=ambient temperature of Jimma which is 19^0C

$h_{vaporization}$- Heat of vaporization of water hfg=2269.86 kJ/kg

$$Eu = 0.4kg * 4.187kJ/kg.k(90.5 - 19)k + (0.4kg - 0.32kg)2269.86kJ/kg$$

$Eu = 300.78kJ$/injera

Taking average family size of five and each will consume three injera per day the total amount of energy utilized will be

Amount of injera required per dayis15 injera, for three days 45 injera

$Eu = 300.78kJ$/injera*45 injera=13,500KJ

Energy required for heating up a baking pan

Heating up energy is the amount of energy required to reach the baking temperature of the injera on the surface of the pan (180^0).

$$Qh = m_{pan}C_{pan}(T_{baking-}T_{room}) \quad (4.2)$$

Where Qh=heating up energy,

m_{pan}=mass of pan (average mass of pan is 7kg) [24]

C_{pan}=heat capacity of pan =0.9kJ/kg. k

T_{baking}=temperature of the baking surface of the pan $180^0 c$

$Qh = 7kg * 0.9kJ/kg.k(180 - 19)k$

$Qh = 1{,}014.3\text{KJ}$

Total amount of energy=Energy utilized +Heating up energy

$$Qt = Eu + Qh \quad (4.3)$$

$$= 1{,}014.3kJ + 13{,}500\text{KJ}$$

$$= 14{,}514.3\text{kJ}$$

But there is loos during baking as well as heating up process so taking 1.2 as factory of safety [25]

$$Total\ amount\ of\ energy = 17{,}417.16\text{kJ}$$

4.2 Design of temporary oil storage tank

Temporary oil storage tank is used to control the fluctuation of temperature on the surface baking pan at the time of pouring batter on the pan and to provide uniform temperature distribution to the pan. So, nanofliud with 4% volume concentration of copper nanoparticle is used to store energy and theoretically temperature of this fluid is maintained at 250^0C.To calculate the volume of storage, thermo physical property of nanofliud is needed. The shape of storage is cylindrical to take the advantage of the shape of pan.

Thermo physical properties of the fluid is calculated as follows;

Density of nanofliud is expressed as; -

$$\rho_{nf} = (1 - \emptyset)\rho_f + \emptyset\rho_p \quad (4.4)$$

Specific heat capacity of nanofliud as; -

$$C_{nf} = \frac{(1-\emptyset)\rho_f C_f + \emptyset\rho_p C_p}{\rho_{nf}} \quad (4.5)$$

Table 4. 1 Thermo physical properties of fluids for oil gallery design

No	Material	Density (kg/m3)	Specific heat (kJ/kg.k)
1	Copper	8875	0.412
2	Thermia oil B	713	2.72
3	Nanofliud	1039.48	1.93

Energy stored =energy required

$$Qt = Mnf * C_{nf}\Delta T \quad (4.6)$$

Where , Qt = amount of energy required= 17,417.16kJ, Mnf=mass of nanofliud

$\Delta T = (Toil - Tamb)$ = (250^0C-19^0C) =231k

$Mnf = 32kg$

For 4% of concentration amount of nanoparticle required is $Mnp = 1.3kg$

Volume of the storage will be calculated by using mass and density of nanofliud

$density = mass/volume$

$$Vnf = Mnf/\rho nf \quad (4.7)$$

$$Vnf = 0.0345m^3$$

Problem occurs during the heating of the oil on the closed system is change on the volume of the oil in the tank. This will Couse break down of the system due to pressure developed during

expansion. To prevent this total volume of the storage will be modified to include volume due to expansion

$$\Delta V = \beta nf Vo \Delta T \quad (4.8)$$

Where

ΔV =Change in volume due to temperature,βnf =Thermal expansion of nanofliud, Vo=start volume,βf =thermal expansion of Thermia oil B= $0.00076k^{-1}$[26],βp=thermal expansion of copper nanoparticle =$0.000051k^{-1}$ [27]

Thermal expression for nanofliud is calculated as

$$\beta nf = \frac{((1-\emptyset)\rho f \beta f + \emptyset \rho p \beta p}{\rho nf} \quad (4.9)$$

$$=9.6 * 10^{-6} k^{-1}$$

$$\Delta V = \beta nf Vo \Delta T = 3.83 * 10^{-5} m^3$$

Total volume of oil gallery

$$VT = \Delta V + Vo = 0.03453\, m^3$$

$$VT = \pi/4 * D^2 * Hg \quad (4.10)$$

Where;-D =diameter of the pan=0.58m, H=height of the storage tank, VT=total volume of the storage

$$Hg = (4 * VT)/(D^2 * \pi) = 13\text{cm}$$

Table 4. 2 dimensions for oil gallery

Parameters	Nano fluid	Thermia oil B
Total volume (m^3)	0.03453	0.0412
Diameter (m)	0.58	0.58
Height (m)	0.12	0.165

Dimensional analysis for Thermia oil was done by following the same procedure.

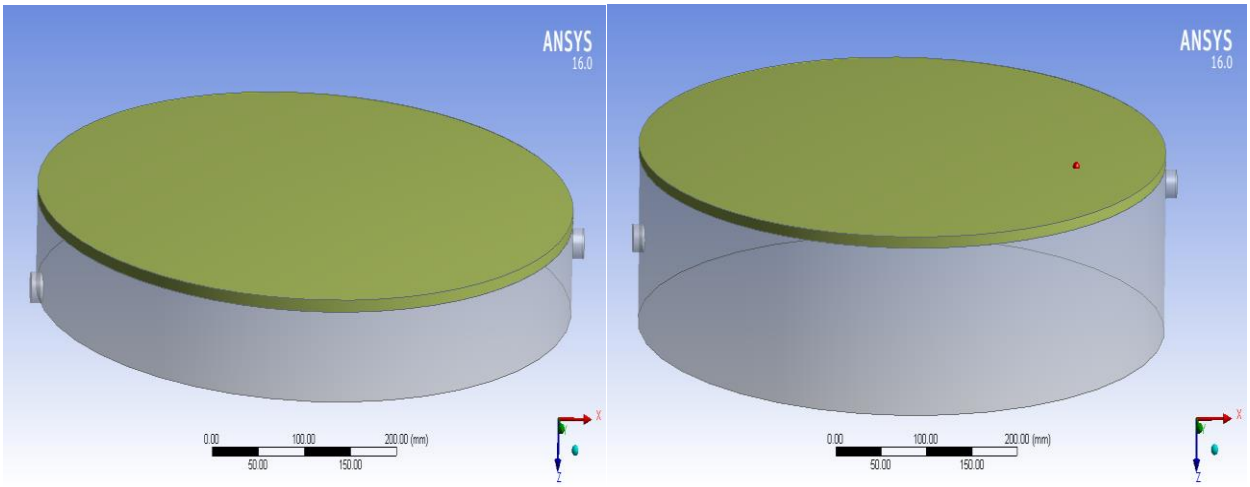

a) b)

Figure 4. 1 a) Oil gallery with Nano fluid b) Oil gallery with Thermia oil B

4.3 Heat transfer coefficient analysis

The top surface of baking pan is exposed to convective and radiation heat transfer with the ambient. So, in order to get heat loss through convection from the pan surface convective heat transfer coefficient will be determined first.

4.3.1 Top surface convection heat transfer coefficient

Convective heat transfer coefficient

$$hc = \frac{NuK}{L} \tag{4.11}$$

Where: hc =convection heat transfer coefficient, Nu =Nusselt number, K =Thermal conductivity

L_c= characteristic length

Some dimensionless parameters are used on the calculation of convective heat transfer coefficient. Those parameters have physical interpretations that relate to conditions in the flow. The flow of heat from the surface of the pan to the ambient is natural.

Reynolds number (Re); - the ratio of inertia to viscous forces in a region of characteristic dimension.

$$Re = \frac{\rho V l}{\mu}. \tag{4.12}$$

From this expression the large value of Reynolds number indicates the domination of inertia force over viscose force and small value implies domination of viscose force over inertia. This number also determines the existence of laminar and turbulent flow.

Prandtl number (Pr); - The ratio of momentum diffusivity (kinematic viscosity) to thermal diffusivity.

$$Pr = \frac{v}{\alpha} \tag{4.13}$$

Where; ν: kinematic viscosity, ν = μ/ρ, (m²/s), α: thermal diffusivity, α =k/ρ Cp, (m²/s), μ: dynamic viscosity (kg/m. s), k: thermal conductivity, (SI units: Wm∗K), Cp: specific heat, (SI units: Jkg∗K)

Grashof number (Gr); provides a measure of the ratio of buoyancy forces to viscous forces in the velocity boundary layer.

$$Gr = \frac{g\beta\Delta TL^3}{v^2} = \frac{\rho^2 g\beta\Delta TL^3}{\mu^2} \tag{4.14}$$

Rayleigh number (Ra); - correlations contain the product of the Grashof number and the Prandtl number.

$$Ra = Gr * Pr \tag{4.15}$$

The simple empirical correlations for the average Nusselt number Nu in natural convection are of the form (29)

$$Nu = hcl/k = C(Gr * Pr)^n = C(Ra)^n \tag{4.16}$$

The values of the constants C and n depend on the geometry of the surface and the flow regime, which is characterized by the range of the Rayleigh number. The value of n is usually ¼ for laminar flow and 1/3 for turbulent flow. The value of the constant C is normally less than 1.

Nusselt number for heat transfer to and from horizontal plat at constant heat flux is experimentally produced as

$$Nu = 0.13(Gr * Pr)^{1/3}) \qquad \text{For GrPr<2*10^8} \tag{4.17}$$

$$Nu = 0.16(Gr * Pr)^{1/3}) \qquad \text{For 2*10^8<GrPr<10^11} \tag{4.18}$$

In these equation all properties except volumetric expansion are evaluated at Te [30]

$$Te = Tpan - 0.25(Tp - Tamb) \quad (4.19)$$

β *will be evaluated at* $Tamb + 0.25(Tp - Tamb)$

$$Te = 180^0C - 0.25(180^0C - 19^0C) = \mathbf{139.75^0C}$$

So, the property of air will be evaluated at this temperature

Then, for β temprature=$19 + 0.25(180 - 19)$=332.25K

$$\beta = 1/T = 1/332.25k = 3 * 10^{-3}/K$$

Properties of air at Te=139.75^0C

Table 4. 3 Properties of air

$T(^0C)$	Density (ρ,kg/m^3)	Thermal conductivity (K,w/m.k)	Thermal diffusivity (α,m^2 /s) 10^{-5}	Dynamic viscosity (μ,kg/m.s) 10^{-5}	Kinematic viscosity(v, m^2/s) 10^{-5}	Prandtl number pr	Specific heat (Cp,j/kg.k)
120	0.8977	0.03235	3.565	2.264	2.522	0.7073	1011
139.75	0.8547	0.03372	3.8938	2.343	2.7422	0.70414	1012.975
140	0.8542	0.03374	3.898	2.345	2.745	0.7041	1013

Characteristic length for circular disk taken as 0.9D where D is the diameter of the pan [30]

Then, dimensionless ***Grashof number*** will be calculated as,

$$\text{Gr}=\frac{\rho^2 g\beta\Delta T L^3}{\mu^2} = \frac{0.8547^2 * 9.81 * 3 * 10^{-3} * 161 * (0.9 * 0.58)^3}{(2.343 * 10^{-5})^2} = 8.96 * 10\text{^}8$$

Rayleigh numbers become:

$$\text{Ra=Gr*Pr}=8.96 * 10\text{^}8 * 0.70414 = 6.31 * 10\text{^}8$$

From the above Nusselt correlation second equation is used to calculate the Nusselt number

$$Nu = 0.16(6.31 * 10\text{^}8)^{1/3}) \quad = \quad 137.23$$

The convective heat transfer coefficient becomes

$$hc = \frac{NuK}{L} = \frac{137.23*0.03372}{0.9*0.58} \text{ W/}m^2\text{. k} = 8.86 \text{ W/}m^2\text{. k}$$

The rate of heat transfer from the surface of the baking pan is combination of convection and radiation. So, the amount of heat lost by radiation from the pan surface will be determined.

Radiation heat transfer coefficient is given as;

$$hr = \varepsilon\sigma(Tp + Tamb)(Tp^2 + Tamb^2) \quad (4.20)$$

Where;hr =Radiation coefficientε =Emissivity of the surface =0.95 [31]σ =Stefan Boltzmann coefficient (5.67x10^-8 W/m2K4)

$$hr = 0.95 * 5.67\text{x}10\text{^} - 8 \text{ W/}m^2\text{K}4(180 + 19)(180^2 + 19^2)$$

hr=0.35 W/m^2. k

Total surface heat transfer coefficient at the top surface will be the summation of convection and radiation heat transfer coefficient.

$h = hc + hr$=0.35W/m^2. k+8.86 w/m^2. k

$\text{h} = 9.21\text{W/}m^2\text{.k}$

4.3.2 Convective heat transfer coefficient for nanofliud on the oil gallery

The properties of nanofliud is obtained at film temperature in order to calculate convective heat transfer coefficient.

$$T_{flm} = \frac{Tnf+Tamb}{2} \quad (4.21)$$

$$= \frac{250^0C+19^0C}{2} = 134.5^0C$$

Table 4. 4 Properties of Thermia oil at134.5^0C

$T(^0C)$	Density (ρ,kg/m^3)	Thermal conductivity(K ,w/m.k)	Kinematic viscosity(v, m^2/s) 10^{-6}	Prandtl number pr	Specific heat (Cp,J/kg.k)	Thermal expansion 1/k	Dynamic viscosity Kg/m.s 10^{-3}
134.5	788.4	0.126	3.49	43.36	2298	0.0008	2.75

Table 4. 5 Properties of copper @134.5^0C

$T(^0C)$	Density (ρ,kg/m^3)	Thermal conductivity(K,w/m.k)	Specific heat (Cp,J/kg.k)	Thermal expansion 1/k
134.5	8907.665	392.504	398.15	0.000051

Thermo physical properties of nanofliud will be calculated by using above tables

a) Thermal conductivity of nanofliud is calculated by using wasp model [46]

$$Knf = Kbf\left[\frac{Kp+2Kbf-2\emptyset(Kbf-Kp)}{Kp+2Kbf+\emptyset(Kbf-Kp)}\right] \quad (4.22)$$

$$\text{Knf} = 0.14\text{W/m. k}$$

b) Density of nanofliud

$$\rho_{nf} = (1-\emptyset)\rho_f + \emptyset\rho_p$$

$$= 1113.1\ \text{Kg/m}^3$$

c) Thermal volumetric expansion will be

$$\beta nf = \frac{(1-\emptyset)\rho f\beta f+\emptyset\rho_p\beta p}{\rho nf} \quad (4.23)$$

=0.00066/k

d) Dynamic viscosity of the nanofliud

$$\mu nf = \frac{\mu_{bf}}{(1-\emptyset)^{2.5}} \quad (4.24)$$

$$\mu\text{nf} = \frac{2.75*10^{-3}\text{kg/m.s}}{(1-0.04)^{2.5}} = 3*10^{-3}kg/m.s$$

e) Specific heat of nanofliud

$$C_{nf} = ((1-\emptyset)\rho_f C_f + \emptyset\rho_p C_p)/(\rho_{nf})$$

$$= 1836\text{J/Kg.k}$$

f) Prandtl number

$$\text{Pr} = \frac{\mu nf * C_{nf}}{\text{Knf}} \quad (4.25)$$

$$= 39.4$$

Table 4. 6 Thermo physical properties of nanofliud

$T(^0C)$	Density (ρ,kg/m^3)	Thermal conductivity(K ,w/m.k)	Prandtl number pr	Specific heat (Cp,J/kg.k)	Thermal expansion 1/k	Dynamic viscosity Kg/m.s 10^{-3}
134.5	950.78	0.14w	38.7	1874	0.00066	2.89

Dimensionless number

$$\text{Gr}=\frac{\rho nf^2 g\beta nf\Delta TL^3}{\mu nf^2}, \quad (4.26)$$

L=Effective length of the heat transfer surface for a horizontal circular plate and can be calculated from the relation [25]

$$\text{Lc}=\frac{A_p}{P} \quad (4.27)$$

Where, A_p= area and P=perimeter of the heat transfer pan surface

$$\text{L}=\frac{\pi D^2}{4\pi D} = \frac{0.58}{4} = 0.145m$$

$$\text{Gr}=\frac{\mathbf{1113.17\ Kg/m3^2} * 9.81m/s2 * 0.00066/k * 231k * (0.145)^3}{\mathbf{3 * 10^{-3} kg/m.s^2}}=6.3*10\text{^}8$$

$$\text{Ra} = \text{Gr} * \text{Pr} = 6.3 * 10^{\mathbf{8}} * 38.7 = 2.5 * 10^{\mathbf{10}}$$

Nusselt number correlation for heated oil on the cylinder is given as

$$Nu = \left[0.825 + \frac{0.387(GrxPr)^{0.1666}}{(1+(0.492/Pr)^{0.5625})\text{^}0.2962}\right]^2 \quad (4.28)$$

=452

Now, convective coefficient of nanofliud on the storage tank becomes

$ho = \frac{NuKnf}{L} = \frac{452*\mathbf{0.14w/m.k}}{0.145m}$=437 W/$m^2$. k

4.4 Comparison of thermo physical property of nanofliud and Thermia oil B

Convective coefficient calculation for Thermia oil B.

Dimensionless number

$$Gr=\frac{\rho^2 g\beta\Delta TL^3}{\mu^2}=\frac{788.4^2*9.81*0.0008*231*0.145^3}{(2.75*10^{-3})^2}=4.54*10^8$$

$$Ra = Gr * Pr=4.54*10^8*43.36=1.96*10^{10}$$

$$Nu = \left[0.825 + \frac{0.387(1.96*10^{10})^{0.1666}}{(1+(0.492/43.36)^{0.5625})\text{^}0.2962}\right]^2 =414$$

$$ho = \frac{NuKnf}{L}=\frac{414*0.126}{0.145}=359.75 \text{ W/}m^2\text{. k}$$

Table 4. 7Comparisons of the analytical results

Property	Nanofliud	Thermia oil	% enhancement
Thermal conductivity w/m.k	0.14	0.126	10
Convective heat transfer coefficient w/m^2.k	437	359.75	17.6

CHAPTER FIVE

DESIGN AND MODELING OF THERMAL STORAGE

5.1 Introduction

This system uses a mixture of sodium nitrate and potassium nitrate as phase change storage material. Selection of this PCM based on the range of operating temperature required by the system (possibility of baking injera on the temperature above$135\ ^0C$). Another types of PCM material have a high melting temperature that requires large area of the collector. This increases the total cost of the system as well as the area of the installation of the system. Based on those criteria's mixture of sodium and potassium nitrite was selected. So the properties required for the design process were obtained from literature.

Table 5. 1 properties of selected salt (PCM)

PCM	Melting temperature(C)	Melting enthalpy (J/g)	Thermal conductivity(w/m.k)		Specific heat capacity (J/g.k)		Density (g/cm^3)
			Solid	Liquid	Solid	liquid	
60%NaNO3 - 40%KNO3	222	100	0.5	0.5	1.42	1.53	1.95

5.2 Dimensional analysis of the storage tank

The amount of heat stored on the PCM equal to the amount of energy required for baking injera

$$Qt = 17{,}417.16\text{KJ}$$

So the storage system will be designed to this amount of energy to meet the energy demand of the baking pan.

Latent energy storing system has three stages

1) Rising of temperature of PCM from ambient to melting point (sensible stage)
2) Melting of PCM at constant temperature (isothermal)
3) Rising of temperature of the PCM up to temperature above melting temperature

Inlet fluid temperature is $Tf = 255^0C$

Melting temperature of PCM $Tm = 222^0C$

Ambient temperature $Tamb = 19^0C$

Melting enthalpy $Hm = 100J/g$

Amount of storage material will be calculated by using above givens

The general equation used for latent heat storage system is given as

$$Q = \int_{Ti}^{Tf} mCpdT \tag{5.1}$$

$$Q = \int_{Ti}^{Tm} mCp_s dT + m\Delta H_m + \int_{Tm}^{Tf} mCp_l dT \tag{5.2}$$

Where; - Cp_s&Cp_l are specific heat capacity at solid and liquid phase

Calculation of total mass of storage medium

i) Latent heat of storage material is

=100k/kg

ii) Amount of heat required for one session is

=17,417.16kJ

iii) Mass of storage medium required for supplying desired amount of heat is

=17417.16KJ/100 kJ/kg

20Kg of salt is considered for the storage

The tank has cylindrical shape

Density of the sodium nitrite is=1950kg/m^3

$$V_{PCM} = \frac{m}{\rho} = \frac{20kg}{1950\text{kg/m3}} = 0.01025m^3$$

Assuming that 20% of volume expansion during heating then final volume will be

$$V_{PCM} = 0.01225m^3$$

Taking the height of the storage as 0.4m the diameter of the cylinder is calculated from the given volume.

$$VT = \pi D^2/4 * H \quad (5.4)$$

$$Dc = \sqrt{\frac{VT*4}{\pi*H}} = 19.54\text{cm}$$

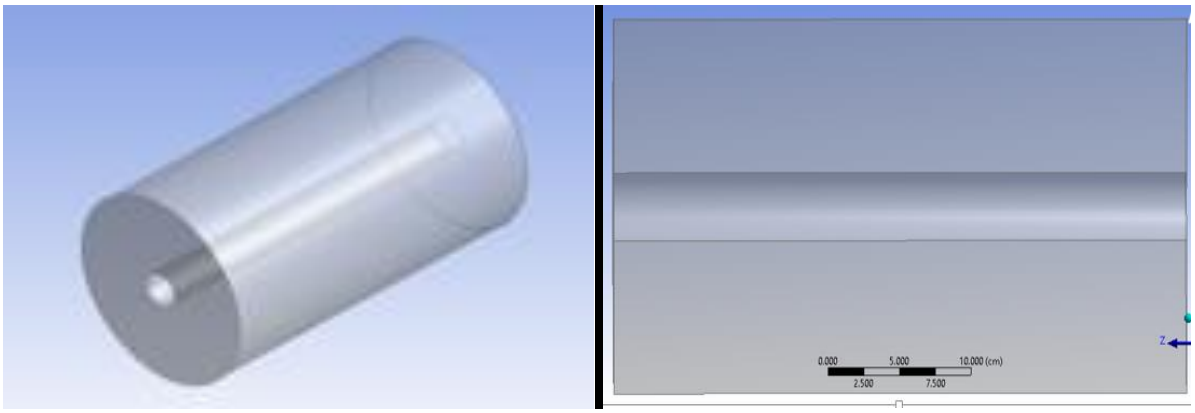

a) b)

Figure 5. 1 a) 3Dmodel of the storage b) Symmetry of the pcm storage

5.3 Numerical modeling

Solidification and melting model on the ANSYS fluent 16.0 is used to model and simulate the melting of PCM.The material was simulated for two different working fluid (nanofluid and Thermia oil B) to compare its fully charging time required. Main parameters that used on this model is liquid fraction (fraction of cell volume which is in liquid form) and mushy zone (which the value of Liquid fraction changes from 0 to 1) [38]. Continuity, mass and energy equations applied to solve the problem. Governing equations used were

Energy equation

$$\frac{\partial(\rho H)}{\partial t} + \bar{V}.(\rho \bar{v}.H) = \bar{V}.(k\bar{v}.T) + S \quad (5.5)$$

The source term, S contains contributions from convection, latent heat transfers due to phase change and any other volumetric heat sources.

Where, H is the enthalpy, ρ is the density, v is the velocity of fluid and S is the source term

The enthalpy H is calculated as the sum of sensible and latent heat.

$$H = h + \Delta H \quad (5.6)$$

Where h is the sensible enthalpy at a point at a given instant of time; ΔH is the latent heat

$$h = h_{ref} + \int_{T_{ref}}^{T} CpdT \quad (5.7)$$

Where h_{ref} is the reference Enthalpy

$Tref$ Is the reference temperature

Cp The specific heat at constant pressure of PCM

$$\Delta H = \beta L \quad (5.8)$$

Where β is the value of liquid fraction and L is the latent heat of PCM. The value of latent heat is zero when material is solid (β=0) and L when material is liquid (β=1).

$\beta = 0$ If $T = Tsolidus$

$\beta = 1$ If $T > Tsolidus$

$\beta = \frac{T - Tsolidus}{Tliquidus - Tsolidus}$ If $Tsolidus < T < Tliqiudus$

Continuity equation

$$\frac{\partial(\rho)}{\partial t} + \bar{V}.(\rho v) = 0 \quad (5.9)$$

Momentum equation

$$\frac{\partial(\rho u)}{\partial t} + \bar{V}.(\rho uu) = \bar{V}\text{p} + \bar{V}(\tau) + \rho g + \text{F} \quad (5.10)$$

Where τ =Stress tensor ρg =the gravitational body force F= the external body forces

5.4 Boundary conditions used for the simulation

Boundary conditions are the set of conditions specified for the behavior of the solution to a set of differential equations at the boundary of its domain. Boundary conditions are important in determining the mathematical solutions to many physical problems. Governing equation used were energy, momentum and continuity equations. Boundary conditions used

- No slip conditions, (At fluid wall interface, there must be no slip)
- Inlet temperature of the fluid (260^0C)
- Inlet mass flow rate (calculated at energy balance on the absorber)
- Outlet was set to outflow (for unknown flow condition) condition
- Interface between the pipe and PCM face was coupled
- Outer wall of the container is insulated so zero heat flux.

Table 5. 2 boundary conditions for PCM simulation

Zones	**Conditions**
Inlet	Mass flow rate
Outlet	Outflow
Outer wall	wall

Assumptions used

- Melting process is transient
- Two dimensional analysis
- thermo physical properties of the HTF and the PCM are constant
- Initial temperature of the system is uniform and the PCM is in the solid phase for melting.
- Inlet temperature and mass flow rate of HTF is constant

CHAPTER SIX

HEAT TRASFER ANALYSIS AND SIZING OF THE PARABOLIC TROUGH COLLECTOR

6.1 Introduction

Design of collector mainly depends on the amount of power required by a given application. For this system sizing of a collector based on the power required for the baking injera. From the previous calculation energy required per injera is 300.78 kJ. Amount of time required to bake one injera is two minutes up to three minutes [32]. Power required will be calculated as follows.

$$\dot{Q} = Eu/\Delta t \qquad (6.1)$$

Taking time required =3minutes=180sec

$\dot{Q} = 300.78\text{KJ}/180sec$=1.671kW

Considering losses through system and taking 1.2 as factor of safety

$\dot{Q} = 2.1\text{kW}$

6.2 Sizing of collector

The size of collector determined by the amount of power required by the application. Schematic of PTC shown on figure 6.1[47].

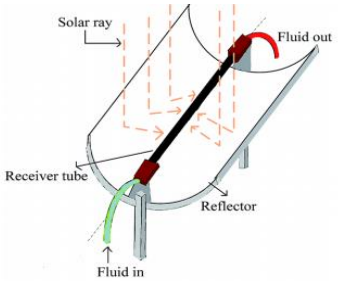

Figure 6.1 Diagram of a parabolic trough collector

Table 6. 1 input parameters for collector design

Parameters	Value	Source
Inlet temperature	170^0C	From outlet of oil gallery
Outlet temperature	260^0C	Fixed
Inner Diameter of the absorber	40mm	From standard of pipe
Diameter of nanoparticle	100nm	High conductivity at smaller size
Receiver temperature	300^0C	For CR of 20 receiver operating tem [39]

6.3 Thermo physical properties of the fluid through absorber

$$T_{flm} = \frac{To+Tin}{2} \quad (6.2)$$

$$=215^0\text{C}$$

Table 6. 2 Thermo physical properties of the fluid through absorber

$T(^0C)$	Density (ρ,kg/m^3)	Thermal conductivity(K,w/m.k)	Specific heat (Cp,J/kg.k)	Thermal expansion 1/k	Dynamic viscosity Kg/m.s 10^{-4}
215	1035	$0.2W$	2230	0.00066	9.6

Mass flow rate through absorber will be calculated from Conservation of enrgy equation for steady flow of fluid flowing througn a tube.

Power required for baking is 2.1KW this amount of power extracted from the collector

$$Qu = \dot{m}Cp(Tout - Tin) \quad (6.3)$$

$$\dot{m} = 0.0123kg/s$$

Heat transfer coefficient calculation

This property of the fluid depends on Nusselt number, Reynolds number, conductivity, peclet number and Prandtl number.

$$Nu_{nf} = \frac{h_{nf}D}{K_{nf}} \tag{6.4}$$

Nusselt number correlation for flow through tube is given as follows [33]

$$Nu_{nf} = 0.4328(1 + 11.285\emptyset^{0.754}{Pe_d}^{0.218}){Re_{nf}}^{0.333}{Pr_{nf}}^{0.4} \quad \textbf{\textit{Laminar}} \tag{6.5}$$

$$Nu_{nf} = 0.0059(1 + 7.6286\emptyset^{0.6886}{Pe_d}^{0.001}){Re_{nf}}^{0.9238}{Pr_{nf}}^{0.4} \quad \textbf{\textit{Turbulent}} \tag{6.6}$$

$$Ped = \frac{u_m d_p}{\alpha_{nf}} \tag{6.7}$$

$$Renf = \frac{u_m D}{\nu_{nf}} \tag{6.8}$$

$$Prnf = \frac{\nu_{nf}}{\alpha_{nf}} \tag{6.9}$$

$$\alpha_{nf} = \frac{k_{nf}}{(\rho c)_{nf}} \tag{6.10}$$

Where; u_m mean velocity of the fluid

d_p Diameter of the nanoparticle

Ped Peclet number

Mean velocity of fluid is calculated from the mass flow rate given above

$$\dot{m} = \rho_{nf} A u_m \tag{6.11}$$

Table 6. 3 Result for the above parameters

Parameters	Reynolds number	Prandtl number	Peclet number	Mean velocity (m/s)
Values	650	18	0.024	0.015

The result on the table shows that flow of the fluid is under laminar regime so Nusselt relation for laminar flow is used

Table 6. 4 Result for Nusselt number and heat transfer coefficient

Parameters	Nusselt number	Heat transfer coefficient (W/m^2.K)
Result	18	65

6.4 Design of length of the absorber

Assumptions

- PTC operate at steady state
- Uniform heat flux over absorber
- Receiver temperature has no great variation along the tube
- There is temperature gradient between receiver and working fluid

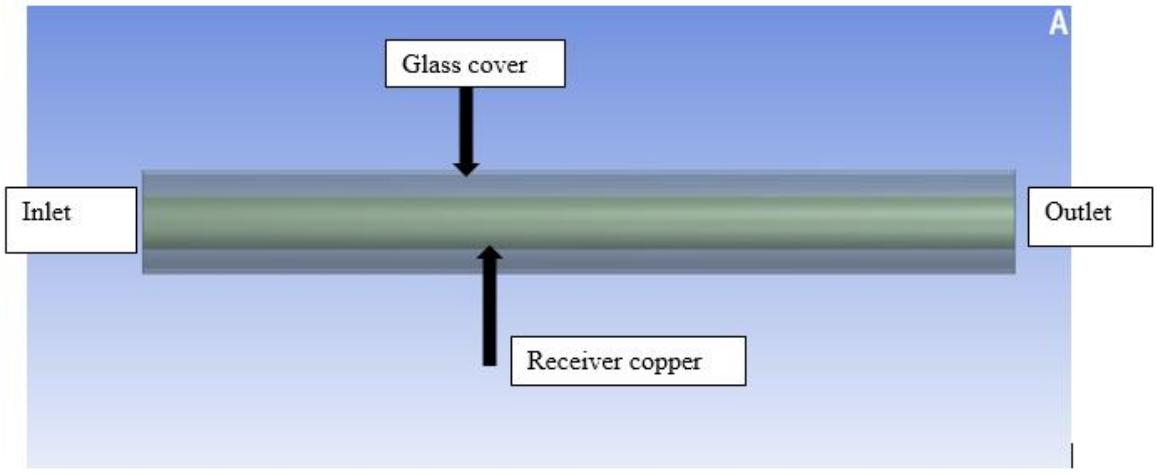

Figure 6. 2 Receiver

Conservation of enrgy equation for steady flow of fluid flowing througn a tube is given as

The surface temprature of reciever is assumed to be constant along the tube . From Newton's law of cooling, the rate of heat transfer to or from a fluid flowing in a tube can be expressed as [29]

$$\dot{Q} = hAr(\Delta Taveg) \quad (6.12)$$

Where $A = heat\ trasfer\ area(\pi DL)$

$\Delta Taveg$=averge temprature difference between fluid and the surface

$\Delta Taveg$ can be approxmatly expressed as arithematic mean temprature difference

$$\Delta Tam = \frac{\Delta Ti + \Delta Te}{2} \tag{6.13}$$

$$\Delta Tin = (\mathrm{Tr} - \mathrm{Tin}) = 130^0 C$$

$$\Delta Te = (\mathrm{Tr} - \mathrm{To}) = 40^0 C$$

$$\Delta Tam = \frac{140^0 C + 10^0 C}{2} = 85^0 C$$

$$Ar = \frac{\dot{Q}}{h\Delta Tam} = 0.34\, m^2$$

Area of recievr is given as

$$Ar = \pi DL \tag{6.14}$$

$$L = Ar/\pi D = 2.5\mathrm{m}$$

Area of the parabola

The available solar energy on the collector aperture is the product of the direct beam solar irradiation and of the collector aperture [35]

$$Qs = Ib * Aa \tag{6.15}$$

Thermal efficiency of the system is given as

$$\eta_{th} = \frac{Qu}{Qs} \tag{6.16}$$

The efficiency range of most solar concentrators is 40%-60% [34]. The concentration ratio for this kind of application is around 20 [45]. Concentration ratio is given as aperture area divided by the area of the receiver. The area of receiver was calculated above so he only unknown parameter was area of the parabola.

$$CR = \frac{\mathrm{A_a}}{\mathrm{A_r}} \tag{6.17}$$

$$Aa = 6.8 m^2$$

Length of the parabolic trough is equal to the length of the absorber

$$Aa = L * W \tag{6.18}$$

$$W = 2.53\text{m}$$

Thus, the thermal efficiency of the collector becomes 49.02%.

6.5 Heat trasfer analysis of absorber

Receiver is made from copper tube with black coating and cover for receiver is from the glass in order to reduce convective loss. The optimum ratio of outer diameter to inner diameter for parabolic trough is approximately 1.1[36]

Table 6. 5Specifications for receiver

Parameters	Value
Receiver outer diameter	44mm
Receiver inner diameter	40mm
Cover outer diameter	70mm
Cover inner diameter	66mm
Emittance and absorbance of receiver	0.17 and 0.89
Reflectance of concentrator (polished aluminum sheet)	0.95
Emittance of cover	0.86
Transmittance of cover	0.95

Heat is trasfered from the reciver surface to inside of cover by convection and radiation then througn cover to the surounding and sky.For the evacuted anuuluse heat trasfer by convection is neglected deu to that absence of heat trasfer meadia.So heat is trasfered deu to only radition

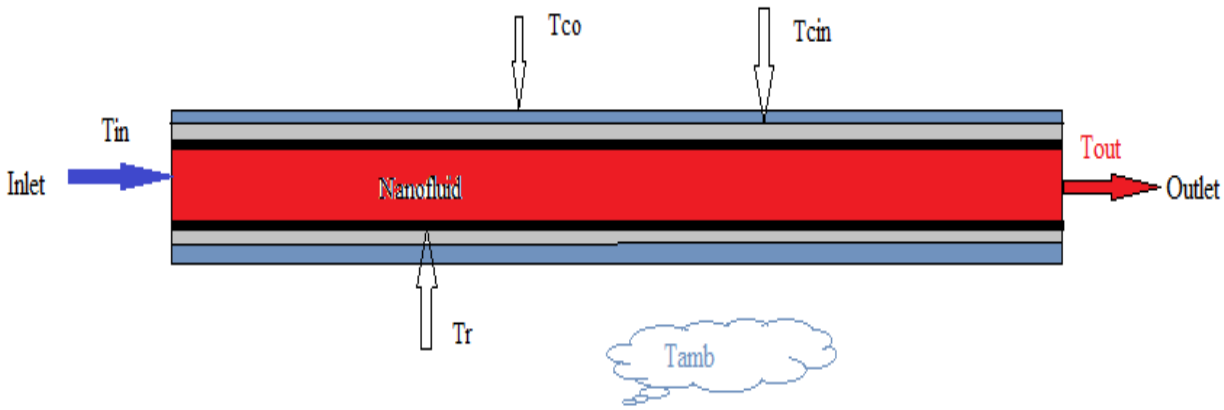

Figure 6. 3 Model for receiver

Heat loss from reciver to the inner surface of cover is given as

$$Qloss = \frac{\pi DrL\sigma[Tr^4 - Tci^4]}{\frac{1}{\varepsilon r} + \frac{1-\varepsilon c}{\varepsilon r}[\frac{Dr}{Dci}]} \quad (6.19)$$

Heat is trasefred from inner surface of cover to the outer by conduction it is given as

$$Qloss = \frac{2\pi kcL[Tci - Tco]}{\ln[\frac{Dco}{Dci}]} \quad (6.20)$$

Heat loss from cover to surrounding and sky is given as

$$Qloss = \pi DcoLh(Tco - Ta) + \varepsilon c\pi DcoL\sigma[Tco^4 - Tsky^4] \quad (6.21)$$

Where ;-Subscript **r** represents the receiver, **ci** and **co** represent the cover inside and outside

kc indicates the cover thermal conductivity=1.4W/m.k, **h** outside concetive coeffiecient (calculated at the average temprature of cover and the ambient)

sky temprature is given as

$$Tsky = 0.0533Tam^{1.5}$$

Reynolds number is calcualted to obtain h value

$$Re = (\frac{\rho VDco}{\mu})air \quad (6.22)$$

V average wind speed =1.4m/s

Then heat trasfer coefficient is obtained from

$$Nu = (\frac{hDco}{k})air \quad (6.23)$$

Nusselt is given for the flow of air acrose tube as

$Nu = 0.4 + 0.54Re^{0.52}$ for 0.1<Re<1000 (6.24)

Nu=$0.3Re^{0.6}$ for 1000<Re<50,000 (6.25)

Assuming that the outer cover temprature much close to the ambiant temprature .

First guess of $Tco = 21^0c$

$Tam = 19^0c$

$Tflm = \frac{Tco+Tam}{2}$=20^0c

Table 6. 6 Property of air at 20^0c

Temprature	Density (kg/m3)	Thermal conductivety(w/m.k)	Dynamic viscocity (kg/m.s)
20^0c	1.204	0.02514	1.825*10^-5

$Re = \frac{\rho VDco}{\mu}$=$\frac{1.204*1.4*0.07}{1.825*10^{-5}}$=6,465.3

Nu=$0.3Re^{0.6}$=$0.3(6{,}465.3)^{0.6}$=58

$h = Nuk/Dco = 20.83W/m^2.k$

Heat loss from cover to ambient and sky will become

$$Q1 = \pi DcoLh(Tco - Ta) + \varepsilon c\pi DcoL\sigma[Tco^4 - Tsky]^4 = 61.87W$$

$$Q1 = \frac{\pi DrL\sigma[Tr^4 - Tci^4]}{\frac{1}{\varepsilon r} + \frac{1-\varepsilon c}{\varepsilon r}[\frac{Dr}{Dci}]} = 61.87W$$

$$Tci = Tco + \frac{Qloss * ln[\frac{Dco}{Dci}]}{2\pi kcL} = 21.060487104118250^0 c$$

$$Q2 = \frac{\pi DrL\sigma[Tr^4 - Tci^4]}{\frac{1}{\varepsilon r} + \frac{1-\varepsilon c}{\varepsilon r}[\frac{Dr}{Dci}]} = 50.4W$$

Heat loss calculated above is compared with original heat loss if they are equal the itration will be stoped here unless another guess is required

Since 61.87W is not equal to 50.4w,so intial guess for outside cover temprature is low

Second guess of $Tco = 23^0 c$

$$Tflm = \frac{Tco + Tam}{2} = 21^0 c$$

Table 6. 7 Property of air at $21\ ^0 c$

Temprature	Density (kg/m3)	Thermal conductivety(w/m.k)	Dynamic viscocity (kg/m.s)
$21^0 c$	1.2	0.025182	1.8285*10^-5

$$Re = \frac{\rho VDco}{\mu} = \frac{1.2 * 1.4 * 0.07}{1.8285 * 10\text{^}-5} = 64315$$

$$Nu = 0.3Re^{0.6} = 0.3(64315)^{0.6} = 57.824071642328770$$

$$h = Nuk/Dco = 20.801796744244612\ W/m^2.k$$

Heat loss from cover to ambient and sky will become

$$Q1 = \pi DcoLh(Tco - Ta) + \varepsilon c\pi DcoL\sigma[Tco^4 - Tsky]^4 = 61.874W$$

$$Q1 = \frac{\pi DrL\sigma[Tr^4 - Tci^4]}{\frac{1}{\varepsilon r} + \frac{1-\varepsilon c}{\varepsilon r}[\frac{Dr}{Dci}]} = 61.874W$$

$$Tci = Tco + \frac{Qloss * ln[\frac{Dco}{Dci}]}{2\pi kcL} = 23.1207880049249470^0$$

$$Q2 = \frac{\pi DrL\sigma[Tr^4 - Tci^4]}{\frac{1}{\varepsilon r} + \frac{1-\varepsilon c}{\varepsilon r}[\frac{Dr}{Dci}]} = 100.65W$$

Heat loss calculated above is compared with original heat loss if they are equal the itration will be stoped here unless another guess is required

Heat loss are not equal so the cover temprature is with in range of $\mathbf{20^0 c\ and\ 23^0 c}$

There is no significant change on the property of the fluid with this range of temprature so the cover temprature is where the difference of two heat loss is zero obtained by using **MATLAB**

Figure 6. 3 Receiver loss comparison

Outside cover temprature at which the two loss differnace become zero will be obtained from the above graph by interpolation. Heat loss at that poitn is **61.87447W** and the outside cover temperature is $\mathbf{21.45841517^0 c}$

6.6 Optical analysis of parabolic trough collector

Factors considered on the geometrical design of the collector are shown on the figure below. [37]

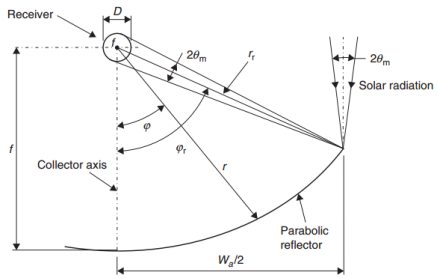

Figure 6. 4 Dimension of PTC

$$r = \frac{2f}{1+cos(\varphi)} \qquad (6.26)$$

φ =Angle between the collector axis and a reflected beam at the focus

At the rim angle radius will be given as

$$r_r = \frac{2f}{1+cos(\boldsymbol{\varphi_r})} \tag{6.27}$$

$$Wa = 4ftan(\boldsymbol{\varphi_r}/2). \tag{6.28}$$

Focal point calculated as

$$f = wa/4tan(\boldsymbol{\varphi_r}/2) \tag{6.29}$$

Another input parameter for the collector sizing is diameter of the absorber commercially available is **40 mm** with intercept factor of **95.5%** [34]. For rim angle $\boldsymbol{\varphi_r = 90^o}$ maximum concentration will occur and optical efficiency is high reflected beam spread is minimized, so that the slope and tracking errors are less pronounced.

Having those parameters, the remaining geometrical parameters of the collector will be calculated

Table 6. 8 Input parameters for collector design

Input parameter	Value	Selection criteria
Rim angle	$\boldsymbol{90^o}$	maximum concentration will occur and optical efficiency is high reflected beam spread is minimized, so that the slope and tracking errors are less pronounced
Intercept factor and receiver diameter	0.995 and 40mm	Commercially available

Table 6. 9 Results

Parameters	Focal point (m)	Rim angle radius (m)
Values	0.62	1.26

CHAPTER SEVEN

ENERGY LOSS ANALYSIS FOR FLOW THROUGH PIPES AND PUMP SELECTION

7.1 Introduction

When fluid flow through the pipe fluid experiences some resistance due to some of energy of fluid lost. When the viscosity of the fluid is taken into account total energy head is no longer constant along the pipe. Due to this loss hydraulic loss was added to the equation of Bernoulli equation. The Bernoulli equation for viscous flow given as;

$$\frac{v1^2}{2g} + \frac{p1}{\rho g} + z1 = \frac{v2^2}{2g} + \frac{p2}{\rho g} + z2 + \Delta h_{ls} \quad (7.1)$$

For horizontal pipe $v1 = v2, z1 = z2$

$$\Delta h_{ls} = \frac{p1-p2}{\rho g} \quad (7.2)$$

For $v1 = v2, z1 \neq z2$,

$$\Delta h_{ls} = \frac{p1-p2}{\rho g} + (z1+z2) \quad (7.3)$$

Friction head (hf) is the sum of major and minor head friction losses on the liquid being moved in pipes, valves and equipment in the system.

Static head is simply the difference in height of the supply and destination reservoirs and it is independent of flow.

Total head is the sum of friction head and static head.

Major head losses; -

$$h_j = \frac{f.L.V^2}{d.2g} \quad (7.4)$$

Where $h_j, loss\ of\ head\ due\ to\ friction$,

f, co-efficient of friction which is a function of Reynolds number

$f = \frac{16}{R_e}$ for $R_e < 2000 (viscouse\ flow)$

$f = \frac{0.079}{{R_e}^{1/4}}$ for $R_e\ varying\ from\ 4000\ to\ 10^6$

LP=length of pipe V=mean velocity of flow, d=diameter of the pipe

Mainor head losses;

Is losses due to different profile of the pipes such as fittings, bends …etc.

$$h_n = \sum \frac{kV^2}{2g} \qquad (7.5)$$

K = Minor loss coefficient read from the table 7.2

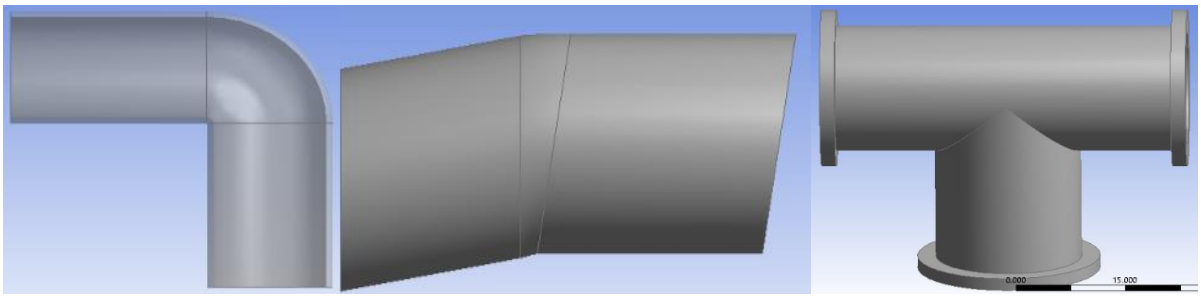

a) *b)* *c)*

Figure 7. 1 *a)* 90^0 elbow b) Slightly rounded c) valve

7.2 Total head calculation for the system

The proposed system conations two pumps pump I used to drive fluid from the oil storage tank up to the pan and charging of the PCM material. Pump II was used for discharging of the PCM and drawing the fluid from the temporary oil storage (oil gallery) up to storage tank. So pumps were selected based on the loops which have highest pressure drop.

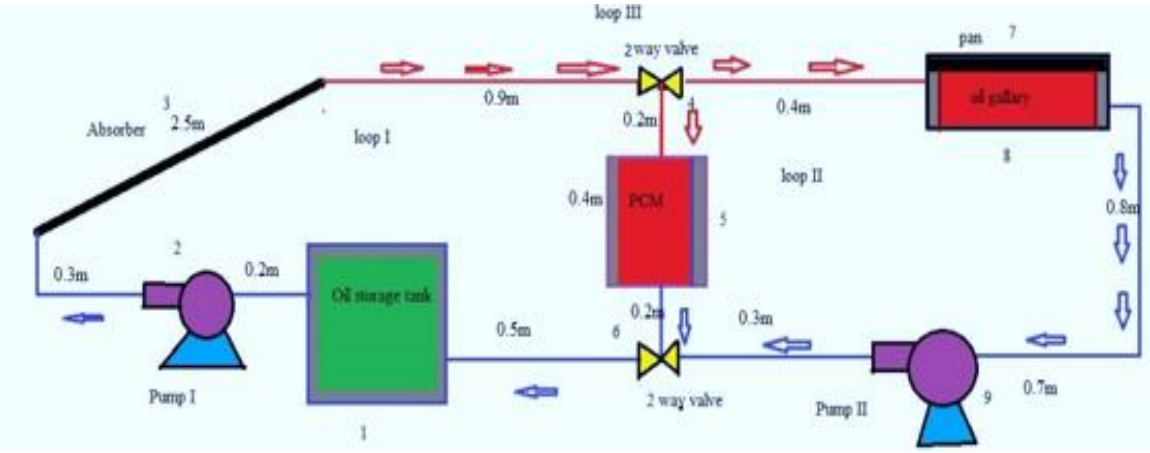

Figure 7. 2 Dimension of pipes

Table 7. 1 Input data for energy loss analysis

Parameters	Values
Viscosity (m/m^2)	3.1*10^-6
Velocity (m/s)	0.0103

$R_e = \frac{Vd}{v}$=150, this value was under laminar flow condition

7.3 Pressure drop and Pump power calculation for pump I

For pump I there were two active loops; loop I and loop III.Therefore the loop with highest pressure drop or head loss was selected to calculate the power input for the pump.

Case 1 for loop III

Effective length for horizontal pipe is=4.3m

This loop have 1 90^0 elbow, 2 slightly rounded bend 1 valves

Table 7. 2 Loss factor for piping system

Types of fitting	Factor (K)
90°elbow	1.75
Gate valve	0.27
Check valve	0.27
Slightly rounded bend	0.12
180° return bend	0.2

Absorber was inclined to $30^0$to the horizontal so, it have pressure drop due to elevation in addition to friction .$L_{abs} = 2.5sin30^0$=1.25m

Major Head loss

$f = \frac{16}{R_e}$=0.1067

$h_j = \frac{f.L.V^2}{d.2g} + L_{abs}$=1.250002667m

Miner head loss

$h_n = \sum \frac{kV^2}{2g}$=1.123mm

Static head was 0.2m

Total head was the summation of above three heads=1.4517893m

Case II for loop I

Effective length for horizontal pipe is=5.4m

Absorber was inclined to $30^0$to the horizontal so, it have pressure drop due to elevation in addition to friction .

$L_{abs} = 2.5sin30^0$=1.25m

Static head =1.2m

This loop have 1 90^0 *elbow , 2 Slightly rounded bend 2 valves*

Major Head loss

$$h_j = \frac{f.L.V^2}{d.2g} + L_{abs} = 1.25077m$$

Minor head loss

$h_n = \sum \frac{kV^2}{2g}$*=1.4mm*

Total head $=h_j + h_n + h_s$=2.26m

So, loop I is used for sizing of the pump I due to it have higher head loss compared with loop III

Pressure loss for all type of flow (laminar transition turbulent horizontal vertical and inclined) was given as; [43]

$$\Delta P = f\frac{L\rho V2}{2d} \qquad (7.6)$$

$$= 0.072bar$$

After determining head loss or pressure loss througn the system amount of pumpe power required to overcomne that loss was selcted

$$P_p = \frac{\rho HgQ}{n_p} \qquad (7.7)$$

Where $P_p = pump\ power\ H\ total\ head\ loss\ Q = volume\ flow\ rate\ , n_p = effeciency\ of\ pump$

$$Q = AV = 1.3 * 10^{-5} m^2/s$$

Assuming efficiency of pump as 50%

$P_p = \frac{\rho HgQ}{n_p}$=0.546w

There for power input of 0.546w was needed to overcome friction developed on *loop I*

7.3 Pressure drop and Pump power calculation for Pump II

Pump two for discharging of PCM material.

Effective length for loop II=1.4m

Static head=1.8m

This loop have 2 90^0 elbow 2 valves

Table 7. 3 Results for pump II

Parameters	Results
Major head loss (mm)	0.204mm
Minor head loss (mm)	2.4mm
Total head loss(mm)	1.8016m
Pump input power(watt)	0.44w
Pressure drop (bar)	*0.0187bar*

CHAPTER EIGHT

RESULTS AND DISCUSSION

This section contains two parts the first one is Injera baking pan simulation results and second part is simulation of PCM.

8.1 CFD results for Injera baking pan for nanofliud and shell Thermia oil as HTF

The simulation for Injera baking pan with temporary oil storage tank is performed on ANSYS (fluent) 16.0 software. The governing equations used for this analysis were energy equations, Continuity equations and momentum equations.

Models

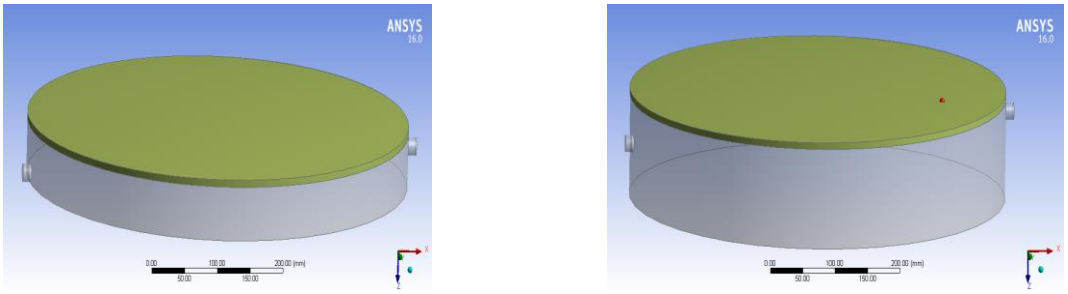

a) b)

Figure 8. 1 a) for nanofliud b) for shell Thermia oil B

Table 8. 1Boundary conditions applied

Boundary	Conditions
Inlet	Mass flow of (0.0123kg/s) and temperature of (250^0C)
Outlet	Outflow
Oil gallery walls	Adiabatic
Pan body	Conduction
Top pan surface	Convection and radiation to the ambient
Interface (pan and fluid)	Convection

8.1.2 Heat up time and Temperature distribution using nanofliud as HTF

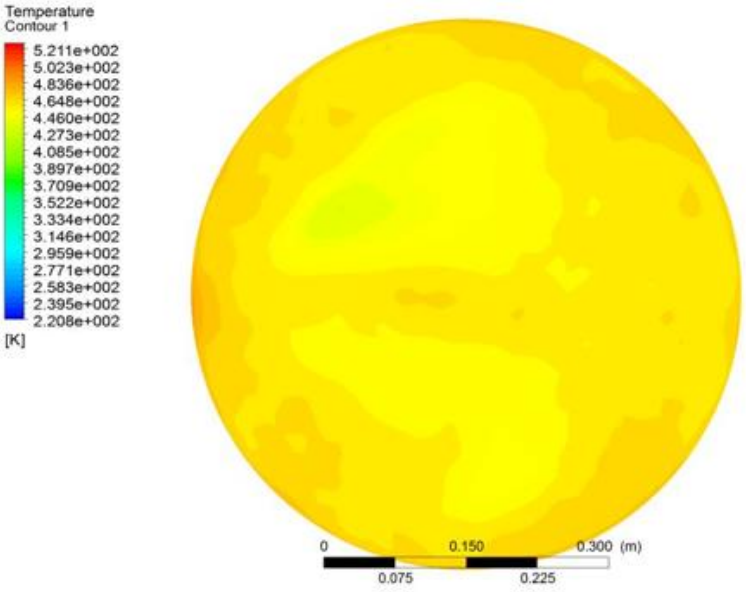

a)

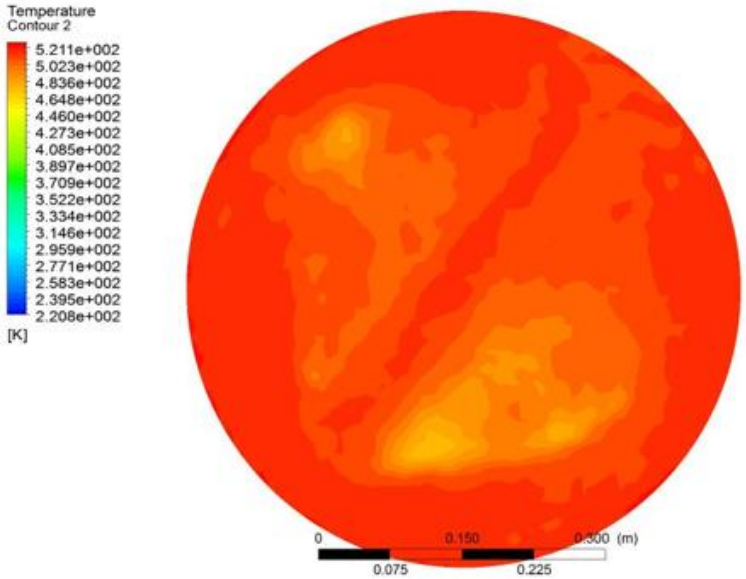

b)

Figure 8. 2Temperature distribution on a) Pan surface b) Oil storage

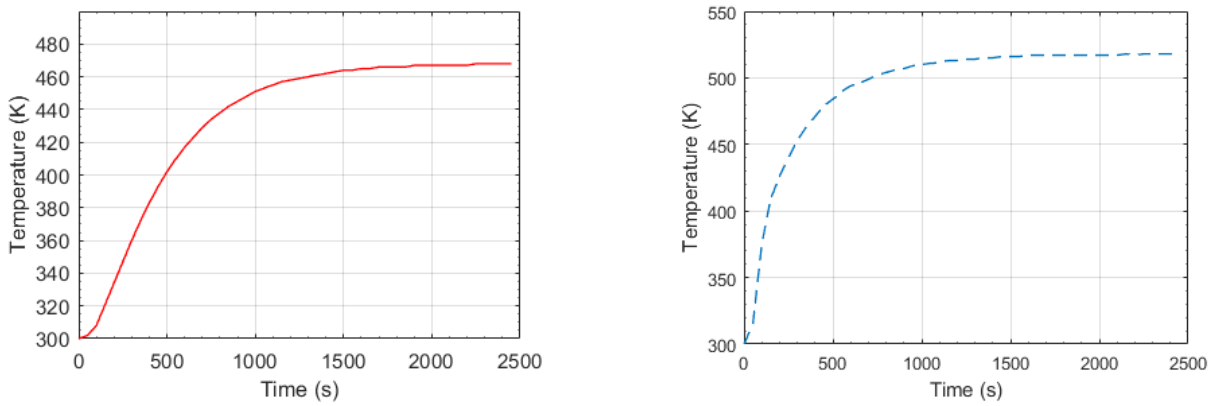

a) b)

Figure 8. 3 Heat up time for; a) Pan b) Oil storage

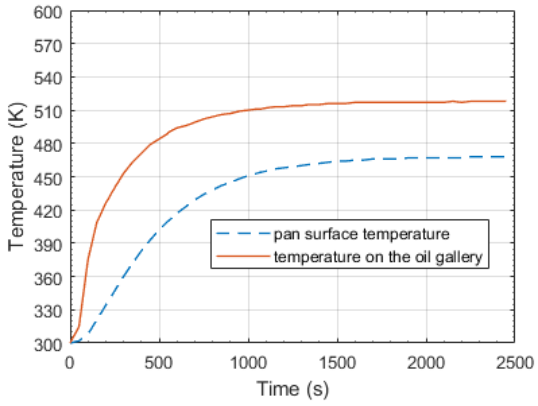

Figure 8. 4 Temperature distribution on oil gallery and surface of pan

Figure (8.3 a) Shown above is the temperature in K versus time in second which shows the time required to reach maximum temperature on the surface of the injera baking pan when the surface of pan exposed to convection and radiation losses from the top and given boundary condition. The maximum temperature obtained at the surface of the pan is 468K (195^0C) and the time required to reach this temperature is 1900sec (31minutes).The pan surface was at the steady condition for this temperature and there is no change for temperature on the surface of the pan as time increase further.

Figure (8.3 b) Shown above also temperature versus time graph for the nanofluid on the oil gallery (temporary oil storage) it shows the maximum temperature of the oil on the gallery with respect to the time required to reach that temperature. The Maximum temperature obtained on the oil gallery was 518K (245^0C) at a time of 1600sec (27minutes).The system was steady beyond this time.

Figure (8.4) shows the temperature of the pan and oil versus time. It shows that at given instant of time the temperature of the oil is greater than that of the pan surface.

The temperature distribution on the baking pan and oil gallery was shown above. From the above contour it was observed that temperature distribution on the surface is more uniform but there was some gradient on the surface due to uneven distribution of heat on the temporary storage.

8.1.3 Heat up time and Temperature distribution using shell Thermia oil B as HTF

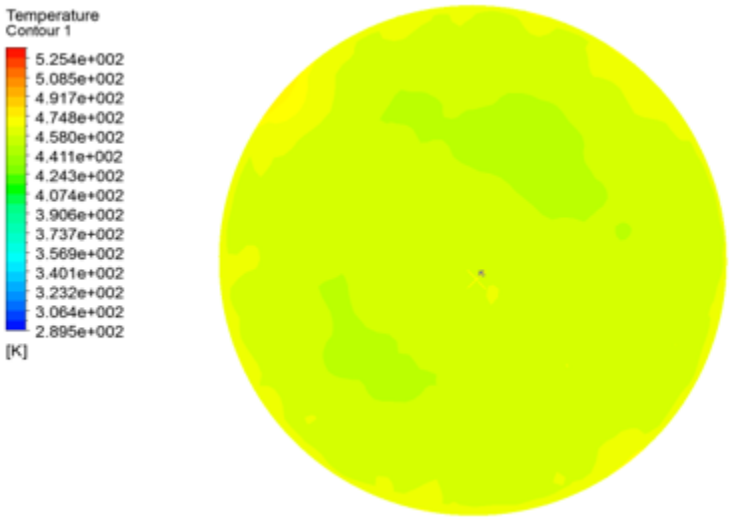

a)

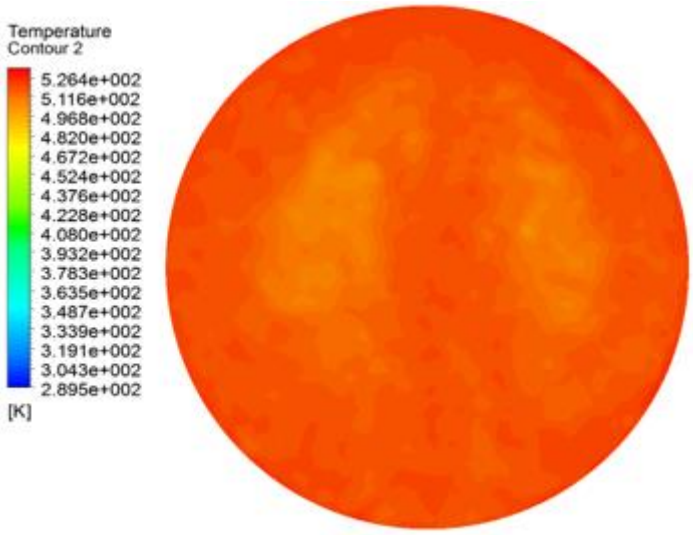

b)

Figure 8. 5Temperature distribution on a) Pan surface b) Oil storage

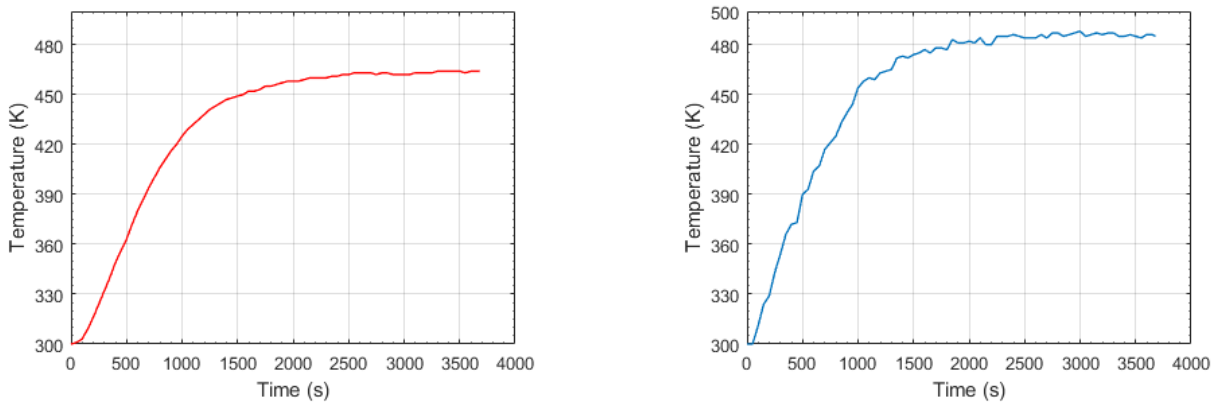

a) b)

Figure 8. 6 Heat up time for; a) Pan b) Oil storage

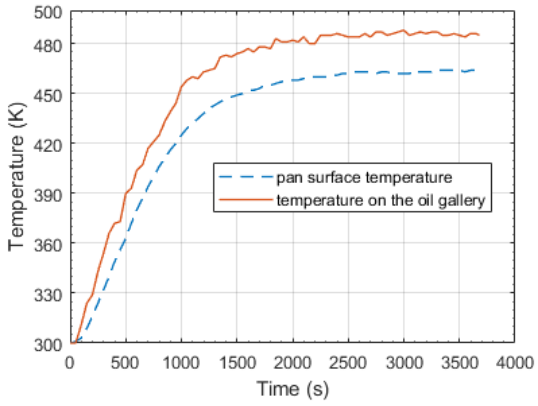

Figure 8. 7 Temperature distribution on oil gallery and surface of pan

Figure (8.6 a) Shown above is temperature in K versus time in second which shows the time required to reach maximum temperature on the surface of the injera baking pan when the surface of pan exposed to convection and radiation losses from the top and given boundary condition. The maximum temperature obtained at the surface of the pan is 464K (191^0C) and the time required to reach this temperature is 3300sec (55minutes).The pan surface was at steady condition for this temperature and there is no change for temperature on the surface of pan as time increase further

Figure (8.6 b) Shown above also temperature versus time graph for the nanofliud on the oil gallery (temporary oil storage) it shows maximum temperature of the oil on the gallery with respect to the

time required to reach that temperature. Maximum temperature obtained on the oil gallery was 487K (214^0C) at time of 2750sec (46minutes).The system was steady beyond this time.

The temperature distribution on the surface of the pan shown on the temperature contour that was not uniform as temperature distribution on the surface of pan using nanofliud as heat transfer media.

Table 8. 2 Simulation results for nanofliud

Parameters	Temperature (o_C)	Time (s)
Temperature on the surface of pan	195	1900
Temperature on the temporary storage	246	1600

Table 8. 3 Simulation results for Thermia oil B

Parameters	Temperature (o_C)	Time (s)
Temperature on the surface of pan	191	3300
Temperature on the temporary storage	215	2750

8.1.4 Comparison of heat transfer for nanofliud with shell Thermia oil B

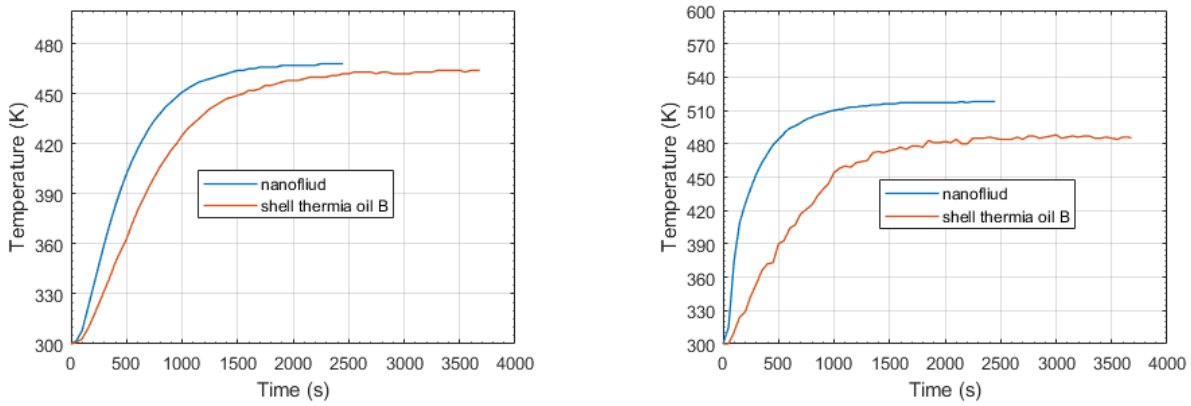

Figure 8. 8 a) Heat up time comparison for pan b) Temperature of fluid on the oil gallery

Figure 8.8 **a)** shows heat up time for Injera baking pan for nanofliud and conventional fluid (shell Thermia oil B) as heat transfer media. From the figure it was observed that time required to heat the surface of the pan is smaller for nanofliud than that of conventional fluid due to its high thermo physical properties. The pan surface have maximum temperature of 195^0C at time of 31 minutes for nanofliud. For shell Thermia oil B the maximum temperature on the surface of pan was 191^0C at time of 55 minutes. For the case of nanofliud, the maximum temperature attained on the surface of pan 191^0C for shell Thermia oil B could be attained at the time of 25 minutes.

*Figure 8.*8 b) shows temperature versus time graph for nanofliud and shell Thermia oil on oil gallery. From the result it was observed that the time required to reach steady state for nanofliud is smaller than that of shell Thermia oil B.

Hence, the system was at steady state after attaining the maximum temperature and the convergence criteria of 10^{-6} for continuity, velocities and energy was used to monitor the solution.

8.2 CFD results phase change material for nanofliud and shell Thermia oil as HTF

The simulation for PCM was performed by ANSYS 16.0 (fluent). Models used were Solidification and melting, energy and laminar flow

Model

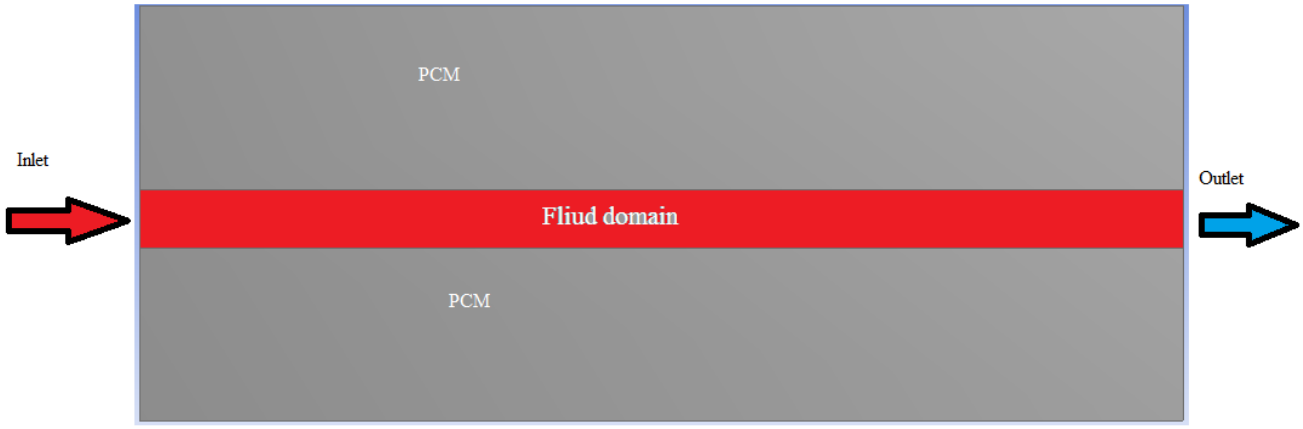

Figure 8. 9 PCM model

Table 8. 4Boundary conditions used

Zones	**Conditions**
Inlet	Mass flow rate (0.0123kg/s) and inlet fluid temperature (255^0C)
Outlet	Outflow
Outer walls	Adiabatic
PCM	Interior

For the PCM heat transfer was by conduction at its solid state and convection at its liquid phase.

Assumptions used

- Melting process is transient
- Two dimensional analysis
- thermo physical properties of the HTF and the PCM are constant
- Initial temperature of the system is uniform and the PCM is in the solid phase for melting.
- Inlet temperature and mass flow rate of HTF is constant

8.2.1 Liquid fraction for PCM using nanofliud as HTF at different time

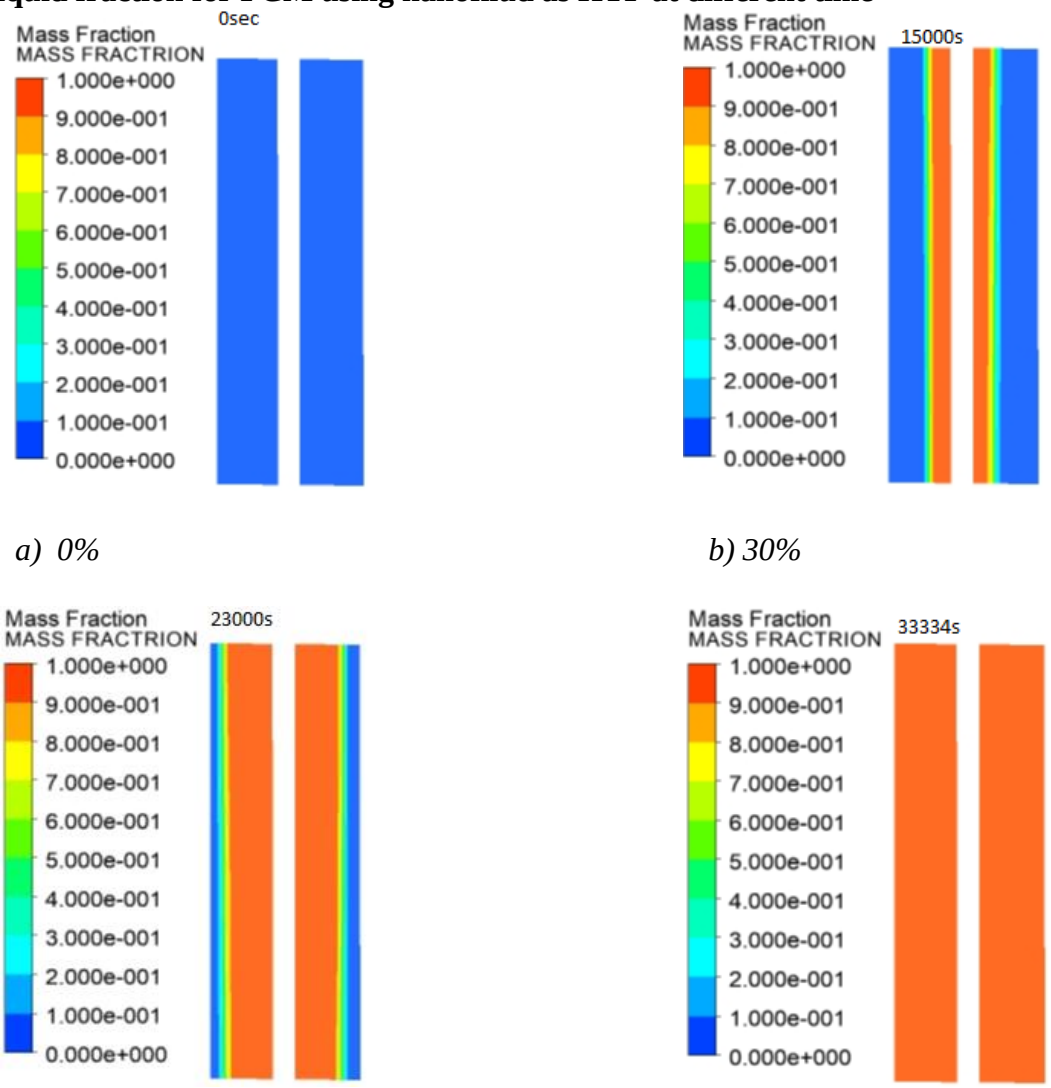

a) 0% *b) 30%*

c) 75% d) 100%

Figure 8. 10 present of mass fraction melted through a given time

The liquid fraction in figure shows amount of PCM that melted (liquid fraction) for a given time. PCM material could melt after absorbing enough amount of energy required to melt. At time 0sec or initially the system was at room temperature so, all PCM was at solid state. Figure b) shows that 30 % of PCM material was melted due to addition of heat to the system at time 15,000sec and after 23,000sec 75% of PCM was melted. The PCM was completely at liquid state after 33,3334sec figure d) shows this condition. The representation of liquid fraction versus time was depicted on the graph.

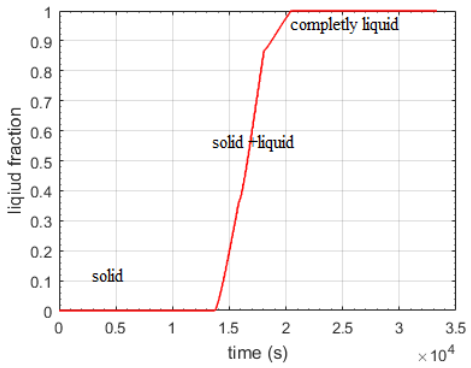

Figure 8. 11 mass fraction versus charging time for pcm using nanofliud

As heat transfer to the PCM the temperature of the material will increase. Initially the PCM absorber sensible energy so its temperature would increase up to melting point of the material. At the melting point it starts to absorber latent form of energy and its temperature would be nearly at constant value. After finishing this stage, it stares to absorber sensible form on energy due to that inlet temperature is greater than that of melting temperature of material

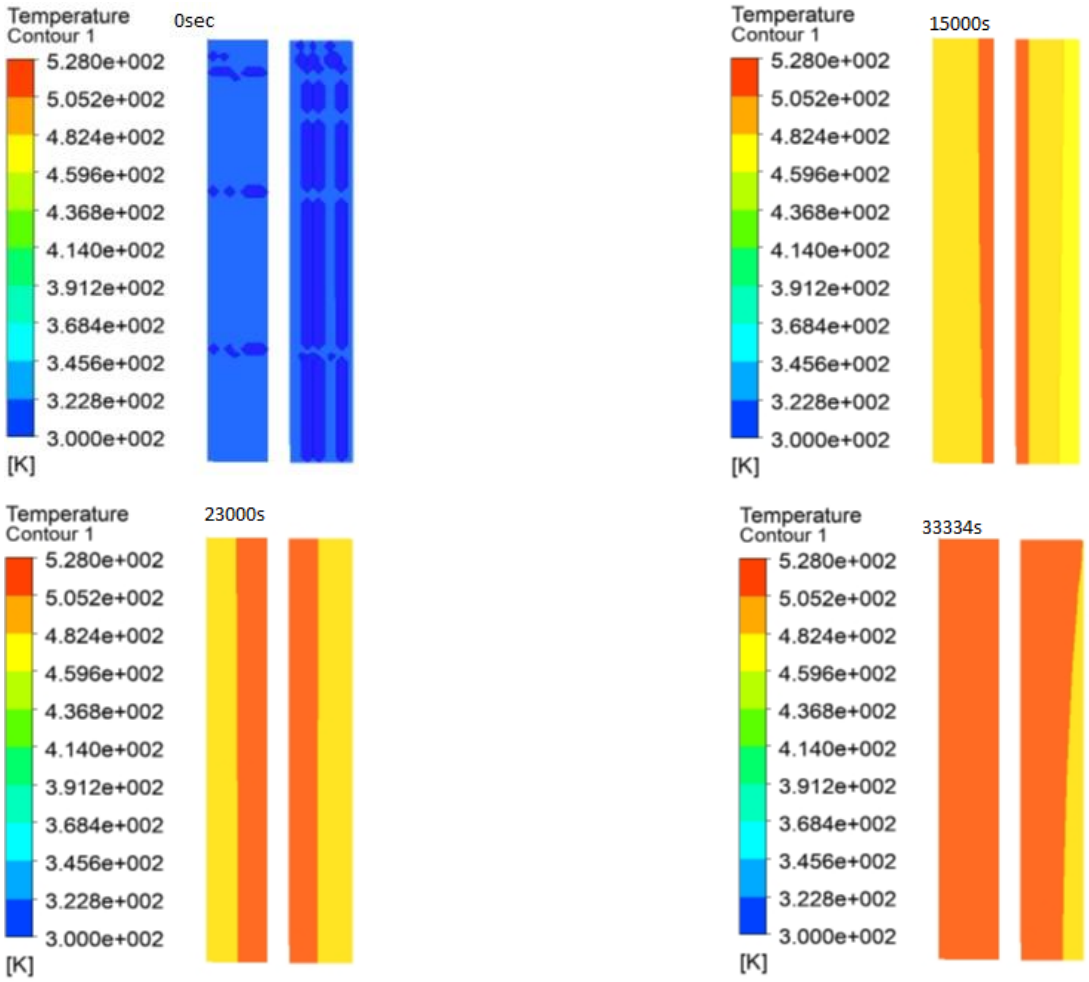

*Figure 8. 12*Temperature contour

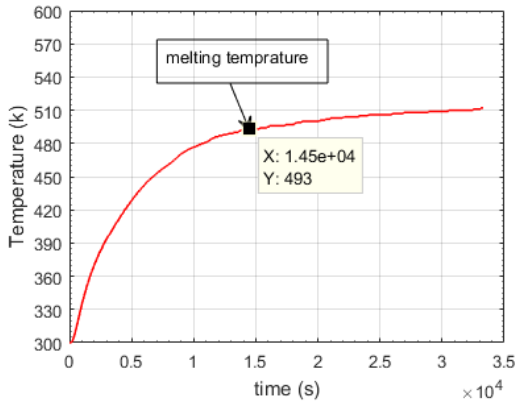

Figure 8. 13 temperature versus charging time for pcm using nanofliud

The inlet temperature of HTF was 528K and theoretical melting temperature of PCM was 495K.Figure above shows temperature versus charging time. From initial point up to the melting point it absorber sensible heat, then it starts to absorb latent heat. Due to high inlet temperature the material would absorbs additional sensible amount of energy. Maximum temperature that stored on the PCM was 512K.

To confer the performance of nanofliud with conventional fluid the same simulation was done for PCM material using shell Thermia oil B and the results were represented graphically below.

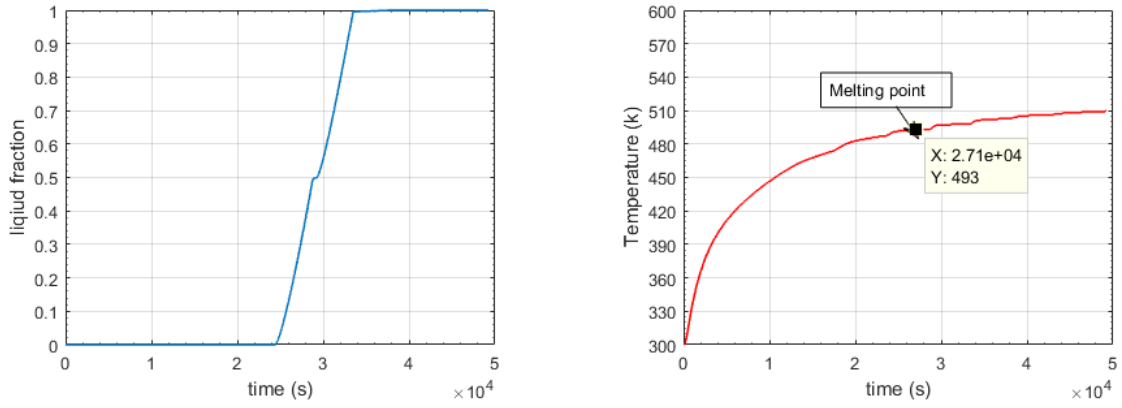

a) *b)*

Figure 8. 14 Charging time for PCM using shell Thermia oil B a) liquid fraction b) Temperature

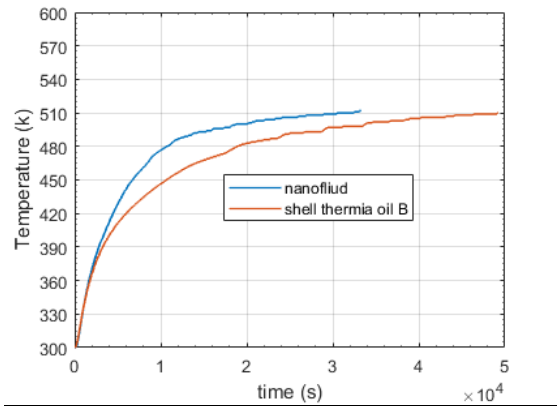

Figure 8. 15 Comparison of charging time based on temperature

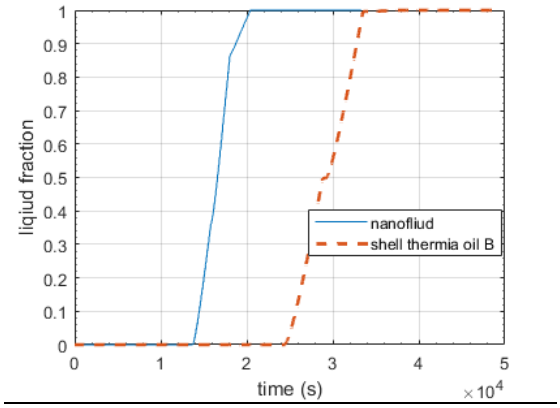

Figure 8. 16 Comparison of charging time based on liquid fraction

Initially the phase change material was at the ambient temperature. When the inlet fluid with temperature of 255^0C pass through the PCM its temperature start to increase. The material has been on solid state until its temperature reach to the melting temperature or absorber enough amount of heat to melt the material. When a material starts to melt, amount of PCM melted was represented by liquid fraction or mass fraction. It absorbs sensible heat up to melting temperature of 222^0C and latent heat at its melting point. Inlet temperature was higher than that of melting temperature of the material, so it absorbs additional amount of energy after melting completely. The simulation on this thesis was performed for two fluids, nanofliud and shell Thermia oil B. The aim of this simulation is to determine the performance of those fluids regards to the time required to charge the material completely. Step by step melting process has been represented by contour for the liquid fraction and temperature for the PCM on the above figures

Using nanofliud as heat transfer fluid, the PCM material start to melt at 13750 seconds (3hrs and 48 minutes). It would be completely liquid state after 33334seconds (9hrs and 15 minutes). The maximum temperature from simulation result obtained was 240^0C.So, it shows that the material stored additional amount of energy at the sensible range.

Using shell Thermia oil B as heat transfer fluid, the PCM material start to melt at 24,900 seconds (6hrs and 54 minutes). It would be completely liquid state after 48,000seconds (13hrs and 18minutes). The maximum temperature from simulation result obtained was 237^0C.So, it shows that the material stored additional amount of energy at the sensible range.

From the above results using nanofliud as heat transfer fluid enhance the charging time required to melt the PCM material and maximum temperature would be stored.

CHAPTER NINE

CONCLUSION AND RECOMMENDATION

9.1 Conclusion

Injera baking method in Ethiopia is the most energy-consuming process. It's main energy sources are firewood, animal dungs, and crop residues. Those energy sources have a great effect on the environment and human being items of environmental degradation and room clean air. Due to this problem, this paper proposes solar energy as an alternative energy source for the Injera baking process. Parabolic trough collector is used as a heat collecting element and heat is transported from PTC to the kitchen by using heat transfer fluid. The proposed system also contains energy storage material that is used for night time baking process.

Global solar radiation for Jimma was calculated from the sunshine hours obtained from the metrology agency. Global solar radiation on the horizontal surface from the calculation was $5.67 kWh/m^2.day$.

Nanofluid used on this paper was Cu/shell Thermia oil B with 4% volumetric concentration and its performance was compared with shell Thermia oil B. Thermophysical properties of the nanofliud calculated by using theoretical models obtained from the literature. From the analytical calculation, the addition of 4% of nanoparticle on base fluid increases thermal conductivity to 10% and convective heat transfer coefficient by 17.6%. The density of the base fluid also increased due to the addition of high density nanoparticle this reduces the size of the system

From the CFD modeling and simulation, the heat up time for the pan and charging time required for the PCM was obtained.

From simulation it was seen that it took 31 minutes to reach a maximum temperature of $195^0\ C$ on the surface of the pan using nanofliud and, it took 55 minutes to reach a maximum temperature of $191^0\ C$ on the surface of the pan. The PCM was fully charged at $9 hrs\ and\ 15 minutes$ with maximum temperature stored on it was $240^0 C$ using nanofliud and it was fully charged at $13 hrs\ and\ 18 minutes$ with maximum temperature stored on it was $237^0 C$ for shell Thermia oil.

The result of this simulation showed that the use of nanofluid reduce heat up time (43.6%) for the baking pan and charging time (30.6%) of the PCM. It also showed that maximum temperature on the system would be obtained by using nanofliud. So, the use of nanofluid as a heat transfer fluid would enhance the system performance.

9.2 Recommendation

Recommendation for the future works are; -

In this paper simulation using the software was performed it is better to develop the system and check its performance experimentally**.** The charging process of PCM requires large time so, some optimization of the storage system is needed.

References

1. Jillian Howell, “Rural Electrification & Renewable Energy in Ethiopia”, Environmental Policy Review 2011.
2. Dagim kebede,” Design and analysis of solar thermal system for hot water supply to minilk ii hospital new building”, June 2016.
3. A. Kalogirou,” Solar thermal collectors and applications”, Progress in Energy and Combustion Science, 30 (2004) 231–295
4. Adem KD, Ambie DA,” A review of injera baking technologies in Ethiopia: Challenges and gaps”, Energy for Sustainable Development. 2017 Dec 1; 41:69-80.
5. Melkamu yaye,” Integration of Scheffler Concentrator and Thermal Storage Device for Indoor Injera”, Addis Ababa university April 2013
6. Hassen AA, Amibe DA, “Nydal OJ. Performance investigation of solar powered Injera baking oven for indoor cooking”, InISES solar world congress 2011 (pp. 186-196).
7. Hassen AA, Kebede SB, Wihib NM, “Design and Manufacturing of thermal energy based Injera baking glass pan”, Energy Procedia. 2016 Aug 1; 93:154-9.
8. Abdulkadir AH, Demiss AA”, Finite element modeling of solar powered injera baking oven for indoor cooking”, Journal of Energy and Power Engineering. 2013;7(6): 1097
9. Asfafaw, T., Mulu, K. and Ole JN, “Design and development of solar thermal Injera baking steam based direct baking” Energy procedia. 2014; volume 57: pages 2946-2955.
10. Tesfay AH, Kahsay MB, Nydal OJ,”Solar powered heat storage for Injera baking in Ethiopia”, Energy Procedia. 2014 Jan 1; 57:1603-12
11. High temperature latent heat thermal energy storage: Phase change materials, design considerations and performance enhancement techniques
12. Mussard M, Nydal O,”Assessments of the thermal storage potential of sensible and latent heat-based systems for solar domestic applications”, InProceedings of the 7th International Renewable Energy Storage Conference 2012.
13. Bianco V, Vafai K, Manca O, Nardini S,” Heat transfer enhancement with nanofliud”, CRC press; 2015 Apr 1
14. Kumar MD, Yuvaraj G, Balaji D, Pravinraj R,” Influence of Nano-Fluid and Receiver Modification in Solar Parabolic Trough Collector Performance”, InIOP Conference Series: Materials Science and Engineering 2018 Feb (Vol. 310, No. 1, p. 012140). IOP Publishing

15. Korres D, Bellos E, Tzivanidis C," Investigation of a nanofluids-based compound parabolic trough solar collector under laminar flow conditions", Applied Thermal Engineering. 2019 Feb 25; 149:366-76.
16. Azari A, Kalbasi M, Rahimi M," CFD and experimental investigation on the heat transfer characteristics of alumina nanofliud under the laminar flow regime. Brazilian Journal of Chemical Engineering", 2014 Jun; 31(2):469-81.
17. Ajay K, Kundan L," Combined Experimental and CFD Investigation of the Parabolic Shaped Solar Collector Utilizing Nanofliud (CuO-H2O and SiO2-H2O) as a Working Fluid",Journal of Engineering. 2016; 2016.
18. Rainer Tamme,Thomas Bauer, Jochen Buschle, Doerte Laing,Hans Mu¨ller-Steinhagen and Wolf-Dieter Steinmann,"Latent heat storage above 120^0C for applications in the industrial process heat sector and solar power generation", International journal of energy research. 2008.
19. Correlation R.A,Arul reja,J.sunil and R.maheswaran,"Estimation of Thermo-Physical Properties of Nano fluids using Theoretical", International Journal of Applied Engineering Research ISSN 0973-4562 Volume 13, Number 10 (2018) pp. 7950-7953.
20. Ching-chang Cho, her-tern you and ching-huang," Numerical Investigation into Natural Convection and Entropy Generation in a Nanofliud-Filled U-Shaped Cavity".
21. P.M.kumar,J.kumar and R.tamilarasan,"Review on nanofliud theoretical thermal conductivity models".
22. Estimation of Global Solar Radiation Using Sunshine and Temperature Based Models for Oko Town in Anambra State, Nigeria.
23. Design of Solar Photovoltaic Power Generation System for Water Pumping
24. G. Alula, T. asmamaw, B. hadush and K. Abdulkadir," Improving energy consumption and durability of the clay bake ware (mitad)", International journal of software and hardware research in engineering. volume 3 November 2013.
25. M.melese," Design and Manufacture of laboratory model for solar powered injera baking oven", November, 2011.
26. Shell Thermia Oil B Paraffinic Mineral Oil for Closed Heat-Transfer Systems
27. Temperature effects on the surface Plasmon resonance in copper nanoparticles
28. Incropera FP, Lavine AS, Bergman TL, DeWitt DP," Fundamentals of heat and mass transfer",Wiley; 2007.
29. Cengel A. "Heat transfer".
30. Holman JP, "Heat transfer", McGraw-hill; 2010.

31. Gashaw Getenet," Heat transfer analysis during the process of injera baking by finite element method", November 2011.
32. Y. melakmu," Integration of Scheffler Concentrator and Thermal Storage Device for Indoor Injera" April 2013
33. A.S. Dalkilic,N. Kayacı,A. Celen,M. Tabatabae, O. Yıldız, W. Daungthongsuk and S. Wongwises,"Forced Convective Heat Transfer of Nanofluids - A Review of the Recent Literature", Current Nanoscience, 2012, 8, 949-969.
34. Ibrahim Ladan Mohammed, "Design and Development of a Parabolic Dish Solar Thermal Cooker".
35. Assessment of the thermal enhancement methods in parabolic trough collectors
36. Performance analysis of solar parabolic trough collector system for different concentration of Al_2o_3 with water as base fluid.
37. Parabolic Trough Technology
38. Vikas, Y.Ankit S.K. Soni," Simulation of Melting Process of a Phase Change Material (PCM) using ANSYS (Fluent)", International Research Journal of Engineering and Technology (IRJET) Volume: 04 Issue: 05 | May -2017
39. John A. Duffie and William A.Beckman," Solar Engineering of Thermal Processes".
40. Asfafaw H. Tesfay, Mulu B. Kahsayand Ole J. Nydal," Steam based charging-discharging of a pcm heat storage".
41. Asfafaw HT, Mulu BK, Ole JN, "Energy Storage Integrated Solar Stove", IEE Global Humanitarian technology conference. 2014
42. Kalogirou SA,"Solar thermal collectors and applications", Progress in energy and combustion science, 2004 Jan 1;30(3):231-95.
43. M.Melese, "Design and manufacture of laboratory model for solar powered injera baking oven", Addis Ababa university, November, 2011.
44. Chamsa-ard W, Brundavanam S, Fung CC, Fawcett D, Poinern G. "Nanofluid types, their synthesis, properties and incorporation in direct solar thermal collectors: A review" Nanomaterials. 2017 Jun;7(6):131.
45. Fernández-García A, Zarza E, Valenzuela L, Pérez M. ''Parabolic-trough solar collectors and their applications'' Renewable and Sustainable Energy Reviews. 2010 Sep 1;14(7):1695-721.
46. Das S. Nanofluids for heat transfer: "An analysis of thermophysical properties". IOSR Journal of Applied Physics. 2015;7(5):34-40.
47. Dabiri S, Rahimi MF. Basic introduction of solar collectors and energy and exergy analysis of a heliostat plant.

Appendix's

Appendix A -Radiation data for the year 2015

months	days	ωs in degree	δ in degree	$\bar{n}$ Hour	$\bar{N}$	φdegree	a	b	Ho J/M2 day	H J/M2 day
1	17	87.08747	-20.9	8.09	11.61166	7.6739	0.347934	0.416433	32059115	20455915
2	47	88.254675	-13	7.05667	11.76729	7.6739	0.316594	0.483771	34567852	20972452
3	75	89.714338	-2.4	8.23333	11.96	7.6739	0.34525	0.422199	36918233	23476107
4	105	91.316749	9.4	7.79667	12.17	7.6739	0.329824	0.455344	38078040	23666973
5	135	92.668222	18.8	6.74667	12.35	7.6739	0.299347	0.520828	37871785	22112171
6	162	93.334163	23.1	4.30667	12.444	7.6739	0.23468	0.65977	37444041	17337201
7	198	93.035113	21.2	5.06333	12.404	7.6739	0.254745	0.616661	37658628	19072830
8	228	91.892589	13.5	4.74667	12.25	7.6739	0.248052	0.631039	38111666	18772641
9	258	90.334749	2.2	6.40333	12.0446	7.6739	0.294614	0.530998	37556681	21666849
10	288	88.73162	-9.6	8.68333	11.83088	7.6739	0.359963	0.390588	35452336	22924782
11	318	87.392802	-18.9	7.19667	11.6523	7.6739	0.322386	0.471326	32752442	20093135

12	344	86.757875	-23	6.73	11.56	7.6739	0.310939	0.49592	31290192	18763289

Appendix B -Radiation data for year 2016

months	days	ωs	δ	$\bar{n}$	$\bar{N}$	a	B	Ho	H
1	17	87.08747	-20.9	7.15	11.61166	0.321786	0.472615	32059115	19645938
2	47	88.254675	-13	7.20667	11.76729	0.320711	0.474925	34567852	21140665
3	75	89.714338	-2.4	7.53667	11.96	0.326436	0.462624	36918233	22814038
4	105	91.316749	9.4	5.02333	12.17	0.256218	0.613495	38078040	19398716
5	135	92.668222	18.8	5.58333	12.35	0.268921	0.586201	37871785	20221171
6	162	93.334163	23.1	4.65	12.444	0.243592	0.640623	37444041	18084581
7	198	93.035113	21.2	3.16333	12.404	0.205269	0.722965	37658628	14673417
8	228	91.892589	13.5	4.64	12.25	0.24524	0.637082	38111666	18543272
9	258	90.334749	2.2	5.75	12.0446	0.277093	0.568642	37556681	20602040
10	288	88.73162	-9.6	8.46333	11.8308	0.353957	0.403493	35452336	22781640
11	318	87.392802	-18.9	7.90333	11.6523	0.341975	0.429238	32752442	20735926
12	344	86.757875	-23	8.25667	11.56	0.353596	0.404267	31290192	20098997

Appendix C- Radiation data for year 2017

Months	Days	ωs	δ	$\bar{n}$	$\bar{N}$	A	b	Ho	H
1	17	87.087	-20.9	9.07	11.61166	0.375194	0.357861	32	21
2	47	88.2545	-13	6.83667	11.76729	0.310555	0.496746	34.56	20.7
3	75	89.7148	-2.4	7.75333	11.96	0.332287	0.450052	36.9	23
4	105	91.3169	9.4	7.98667	12.17	0.334867	0.444509	38	23.86
5	135	92.6682	18.8	6.12667	12.35	0.283131	0.555669	37.87	21.16
6	162	93.3343	23.1	5.97333	12.444	0.277941	0.566821	37.44	20.6
7	198	93.0353	21.2	3.23667	12.404	0.207178	0.718862	37.65	14.867
8	228	91.8929	13.5	3.99	12.25	0.228101	0.673907	38.2	17
9	258	90.3349	2.2	5.15333	12.0446	0.261092	0.603022	37.6	19.5
10	288	88.7316	-9.6	6.62333	11.83088	0.303722	0.511428	35.5	21
11	318	87.3922	-18.9	7.55	11.6523	0.33218	0.450282	32.75	20.4
12	344	86.757875	-23	8.66333	11.56	0.364959	0.379853	31.3	20.32

Appendix D -Table of Thermo physical properties of shell Thermia oil B [31]

Temperature (℃)	Density (kg/m^3)	Specific heat ($kJ/kg.K$)	Thermal conductivity ($W/m.K$)	Kinematic viscosity ($10^{-6} \times m^2/s$)	Prandtle number
0	876	1.809	0.136	230	3375
20	863	1.882	0.134	-	919
40	850	1.954	0.133	25	375
60	837	2.027	0.131	18.2	273
80	824	2.100	0.129	11.5	171
100	811	2.173	0.128	4.7	69
120	797.8	2.246	0.127	-	54
150	778	2.355	0.125	-	32
200	746	2.538	0.121	1.2	20
250	713	2.720	0.118	-	14
300	681	2.902	0.114	0.5	11
320	668	2.975	0.113	-	10
340	655	3.048	0.111	-	9

Appendix E -Table of Thermal Conductivity (W/m.K)], Specific Heat [(J/kg.K)] and density (kg/m^3) of copper

T(k)	*k*	*c*	*ρ*
200	237	798	9000
300	237	903	8960
400	240	949	8910
500	236	996	8870
600	231	1033	8820
800	218	1146	8710

Appendix F -Suggested correlation of daily diffusion fraction with KT

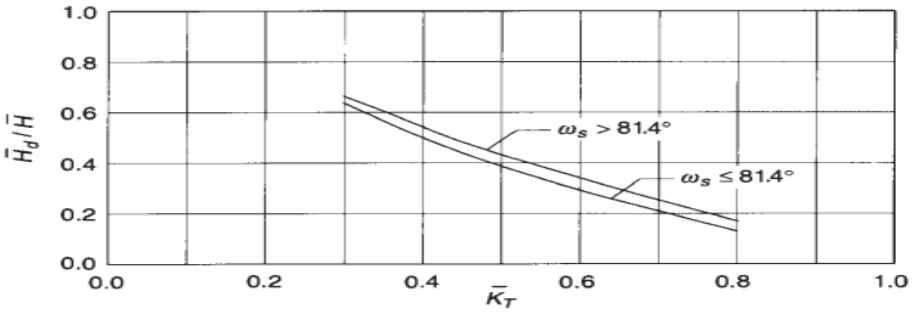

Appendix G -MATLAB code for loss calculation

```
% parabolic trougn collector loss calculation
% input parameteres
Dro=0.044;
Dri=0.04;
Dco=0.07;
L=5.5;
Tco=[21: 0.01: 22];
kc=1.4;
ka=0.02514;
Ta=19;
Tr=310;
sgma=5.67.*10.^-8;
Tsky=0.0533.*Ta.^1.5;
Dci=0.066;
er=0.17; %emitance of reciever
ea=0.89; % absorbance of recievr
r=0.95; %reflectivity
ec=0.86;% emitanceof cover
t=0.95;%trasmitanec of cover
v=1.4;     %speed of air
rho=1.204 ;   % density
mw= 1.825.*10.^-5 ;      %viscocity
Re=rho.*Dco.*v/mw;
Nu=  0.3.*Re.^0.6;           %nusselt number
h= Nu.*ka./Dco;      % convective coefieint
Q1=pi.*Dco.*L.*h.*(Tco-Ta)+ec.*pi.*Dco.*L.*sgma.*(Tco.^4-Tsky.^4);
Tci=0.0012.*Q1+Tco;
Q2=6.7.*10.^-9.*(Tr.^4-Tci.^4);
y=Q2-Q1;
```

```
plot(Q1,Tco,'-',Q2,Tco,'-');
title ("loss comparision")
xlabel("losses ")
ylabel("outside cover temprature")
legend('Q1','Q2')
grid on
```